

Dear editor,

we would like to thank you for having supported a very constructive review of our manuscript. We do believe that the work has improved significantly.

5 Please, find below our point-by-point responses to the reviews (as published on 6 May 2016). These include: (I) comments from Referees (in Bold), (II) author's response (plain text), (III) author's changes in manuscript (in Italic).

All relevant changes made in the manuscript are showed in the marked-up manuscript version attached at the end of this document.

10 1 Referee 1

(I) Comment from Referee:

1. BrC is mainly composed of aged OA

This is one of the main conclusions in this paper. The authors arrive at this conclusion based on the correlations they found between AAE and OA-to-BC ratio, and between AAE and f_{44} . The premise that this conclusion is based on is that AAE is an indicator of how brown the aerosol is. This is not accurate. AAE is an indicator of the wavelength-dependence of absorption. What is more "brown" OA with MAC=2 m²/g (at 532nm) and AAE=2, or OA with MAC=0.2m²/g (at 532nm) and AAE=4? Probably the brownest OA reported in the literature is that observed by Alexander et al. (Science 321, 833-836 [2008]), and it had relatively small AAE. So, with their current analysis, the authors can only make conclusions on the wavelength-dependence of OA absorption, and not on how brown the OA is. However, even this needs further analysis to be convincing. The authors base their analysis on the AAE of the whole aerosol (including both BC and OA). The AAE of the aerosol is dictated by the relative contribution of the components (and coating effects, which we can set aside for now). The increase of AAE with increasing OA-to-BC ratio does not necessarily mean that the added OA upon aging has a larger AAE, it can simply mean that the relative contribution of BC to AAE gets smaller, so the overall AAE increases. In other words, fresh and aged OA could have similar AAE, and the increase in AAE vs OA-to-BC ratio is simply due to the decreased contribution of BC.

(II) Author's response.

30 We agree that the conclusion **BrC is mainly composed of aged OA** is not accurate. In fact, we conversely concluded (and this is stressed in the revised manuscript) that: (i) *we observed the bulk nondust aerosol having the strongest spectral dependence of light absorption (AAE=2.5–6);* (ii) AAEs of this aerosol indicate that it has brown color, but *not necessarily that it equates to brown carbon*; (iii) this aerosol with brown color is defined "brown" aerosol; (iv) *this "brown" aerosol has a secondary origin, large concentrations of organic aerosol (OA), high OA-to-BC ratios, and is dominated by accumulation mode particles.* We revised the manuscript accordingly.

(III) Changes in manuscript.

(*) We modified the title: *Characteristics of brown aerosol in the urban Po Valley atmosphere*

40 (*) In Sect. 4.1, we stressed that the secondary origin of the "brown" aerosol is inferred from *a strong correlation found with the droplet mode aerosol type, a submode of accumulation mode aerosol particles which is by definition secondary in origin* (formed through secondary processes in the atmosphere). This conclusion is reinforced by the correlation with f_{44} .

(*) In Sect. 4.1, we stressed that the correlation with the droplet mode aerosol *gives insights into the likely formation process of this "brown" aerosol.*

45 (*) In Sect. 5.3, we stressed that there are indications that *this "brown" aerosol contains aged OA.* Thus, we speculate *into aged brown OA formation processes.*

(*) In Sect. 5.1, we stressed that we did not directly measure the AAE of OA, but *the AAE of the bulk dust-free aerosol, including both BC and OA contributions (AAE_{BC,OA}).* Changes in this AAE are due to changes in *relative proportions of BC and OA.* This was already illustrated in former Figure 3b of the manuscript, where AAE did not linearly decrease with decreasing f_{BC} . We added

Supplementary Figure 1 showing relative contributions of OA (data color) and BC (data size) on AAE.

(*) In Sect. 5.1, we stressed that our findings indicate *patterns (not absolute values) of AAE_{OA}* , found to *increase with decreasing BC-to-OA, similarly to what observed by Saleh et al. (2014) and Lu et al. (2015)*. To this purpose, we added Supplementary figure 2 showing AAE measured (i.e., $AAE_{BC,OA}$) together with AAE used to calculate BC (AAE_{BC}) in the AAE vs BC-to-OA chart.

(*) Our findings indicate *patterns (not absolute values) of AAE_{OA}* , found to *increase with decreasing BC-to-OA, similarly to what observed by ? and ?*. To this purpose, we added the following Supplementary figure (Fig. 6 here) showing AAE measured (i.e., $AAE_{BC,OA}$) together with AAE used to calculate BC (AAE_{BC}) in the AAE vs BC-to-OA chart.

(I) Comment from Referee:

2. Validity of PSAP measurements and BC concentration calculations.

Figure 4 and figure 6 show that AAE is 2 at BC-to-OA ratio of 20. This puts in question the validity of AAE retrieved from the measurements because at such large BC-to-OA ratio, the particles should have AAE closer to 1. The authors should address this issue to determine whether there is something wrong with the calculations or the measurements that resulted in this factor of 2 overestimation of AAE. Also, BC concentrations are largely underestimated because the calculations (section 3.1) rely on the assumption that AAE of BC is equal to 1 (which is not the case, as retrieved from the instrument in this study). Consequently, the fractions of the different components should be recalculated.

(II) Author's response.

We agree that this important issue was not illustrated enough, and revised the manuscript accordingly to include: (i) PSAP measurement uncertainty (Sect.2.2), and (ii) BC mass concentration calculation method and resulting uncertainty (Sect.3.1); (iii) these uncertainties in relevant figures; and (iv) the explanation that (Sect.4.1) the low AAE values the referee refers to, can be due to these uncertainties and relevant (low) OA values.

(III) Changes in manuscript.

(i) BC was calculated from PSAP-derived absorption coefficients (σ_a), relevant uncertainties *deriving from a number of measurement artifacts*. We referenced previous works in literature which have developed correction algorithms to overcome these artifacts, and mentioned that, based on Virkkula et al. (2010)'s correction, σ_a uncertainty is $\frac{\delta(\sigma_a)}{\sigma_a} = 0.2$.

(ii) *BC mass concentration was calculated using the AAE_{BC} attribution method*. This method assumes a known value of AAE_{BC} at 530-660 nm. This value is commonly set to 1 for externally mixed BC. We referenced previous works in literature, in particular Lack and Langridge (2013) and references therein, which have showed this AAE_{BC} to be (i) larger than 1 for BC aerosol in ambient air (including both internally and externally mixed BC); (ii) for externally mixed BC, 1 for particles with diameter < 50 nm, and 0.8–1.1 for diameters of 50-200 nm; (iii) 0.55–1.7 for internally mixed BC, depending on particle size, coating, core, wavelengths. Based on these previous works, we used $AAE_{BC}=1.1$, and $\frac{\delta(AAE_{BC})}{AAE_{BC}}=0.22$.

(iii) Figure 4 was revised. Both this figure and Suppl. Fig.1, include BC and AAE uncertainties, calculated propagating these σ_a and AAE_{BC} uncertainties.

(iv) We explained *the small trend of the lower AAE values toward 1.5* considering: (i) uncertainties before mentioned, and (ii) OA values (>0) these low AAE values are at. On one hand, Fig.1 shows that AAE values from 1 to 2 are within measurement uncertainties. On the other hand, OA values > 0 in Suppl. Fig.5 suggest that there may have been *spectrally light absorbing material that the AMS cannot detect (refractory material, or material in particles smaller than 100 nm and larger than 1 μ m)* causing a bias in AAE toward values larger than 1. We referenced previous papers in literature discussing this topic. In particular, Lack et al. (2008) analyzed the "bias in filter-based aerosol light absorption measurements due to organic aerosol loading", and found that "at low OA concentrations" (similar to OA concentrations here), "where HOA was a larger fraction of the OA,

PSAP-derived AAE did display a small upward trend to ~ 1.5 , suggesting that the HOA measured may be mildly absorbing".

(I) Comment from Referee:

P1 L15: What's the difference between brown OA and brown carbon?

(II) Author's response.

The referee is right for questioning this. The lack of a common definition for brown carbon causes confusion. We do believe that the scientific community should address this question.

(I) Comment from Referee:

P2 L1: What do you mean by "moderately volatile"? Also, how do you support this claim?

(II) Author's response.

We referred to the classification proposed by Pöschl (2003) - Figure 1 of their paper. In the revised manuscript, we referenced this work.

(III) Changes in manuscript.

We explained in the Introduction section that *there is a gradual decrease of thermochemical refractiveness and specific optical absorption going from BC/EC graphite-like structures to non-refractive and colorless OC. Also, there is a gradual decrease in the volatility from BC (the lowest volatility), to colorless non-refractory volatile OC (the highest volatility). A broad range of coloured organic compounds, with volatility in between these two extremes, have recently emerged*.

(I) Comment from Referee:

P5 L12: "we fixed threshold"? please explain.

(II) Author's response.

We explained the method in the revised manuscript. And finally said that we used this method to identify cases when the aerosol was dominated by dust, and eliminate them.

(III) Changes in manuscript.

In Par.3.1 we explained that: *dust-free aerosol conditions were identified based on the analysis of aerosol spectral optical properties*. We referenced previous works in literature, which have used this analysis to gather information on aerosol type. Among these, Costabile et al. (2013) showed that *the aerosol dominated by dust can be unambiguously identified based on the following combination of SAE, AAE, SSA, and dSSA: $SSA_{530} > 0.85$, $SAE_{467-660} < 0.5$, $AAE_{467-660} \sim 2$, $dSSA_{660-467} = 0.05-0.3$* .

(I) Comment from Referee:

P6 L24: It is not clear why this assumption is needed or whether it is valid. You need more than "mass scales with volume" to justify this assumption

(II) Author's response.

We agree that this assumption is not needed, and:

(III) Changes in manuscript.

we deleted lines at P6L23-28 to avoid unnecessary text.

(I) Comment from Referee:

P7 top paragraph: What are PC2 and PC4? What would be in the primary aerosol that has modes 20-100 nm and 10-40 nm? One would expect those to be BC particles.

(II) Author's response.

The referee is right for noting that PC2 and PC4 are both BC primary aerosols. However, their source is different (probably, heating and traffic emissions, respectively). We revised relevant text.

(III) Changes in manuscript.

(*) We added Supplementary Figure 3, to illustrate weekly diurnal cycles, and loadings of PC1-4.

(*) We clarified (P7L3-5) that *PC1, PC2, and PC4 are BC primary aerosols (all correlated to BC and f_{BC}). PC1 and PC4 are both sourced by traffic emissions, diurnal cycles peaking at rush*

hours and week-days. PC1 is a fine mode aerosol component (PNSD mode peaking from 100 to 200 nm), PC4 an ultrafine aerosol component (PNSD peaking from 20 to 40 nm). PC2 is an ultrafine BC aerosol component, as PC4. Unlike PC4, however, PC2 higher scores are at night-time, and there is no weekly cycle and no peak at "rush hours": PC2 is probably sourced by heating emissions.

(I) Comment from Referee:

Section 5.1: The authors mention that they will compare results with Shinozuka et al. (2009) Russell et al. (2010), Arola et al. (2011), Saleh et al. (2014), and Lu et al. (2015) but only show comparison with Russell et al. and Saleh et al.

(II) Author's response.

These comparisons (both reinforcing our findings) were missing, indeed. We revised Sect.5.1 accordingly.

(III) Changes in manuscript.

(*) Shinozuka et al. (2009)'s results were added in panel a of the revised Figure 6. Relevant data for SSA bins of 0.90-0.92, 0.96-0.98 and 0.98-1.00 were indicated by grey lines.

(*) Lu et al. (2015)'s results were added by grey line in panel c of the revised Figure 6. It was indicated that y-axis of both Lu et al. (2015)'s and Saleh et al (2014)'s results refers to AAE_{OA} , while y-axis of our figure refers to AAE from both BC and OA contributions.

(*) We added that *values of $AAE > 3.5$ are at $SSA > 0.98$, consistent with Shinozuka et al. (2009)'s results at $SSA = 0.98-1.00$. We added that this comparison ultimately shows consistency of "brown" aerosol properties measured in situ at the ground and observed from airborne and AERONET.*

(*) Although we are consistent with Arola et al. (2011)'s findings, the comparison in Fig.6 with their work is not possible. They used absorbing OC column concentrations [$mg\ m^{-2}$] in the x-axis, whereas we show f_{OA} derived from in situ ground measurements. We therefore did not reference this work.

(I) Comment from Referee:

Section 5.1: The AAE values in this study are much larger than Russell et al., especially at low f_{OA} values. I believe this is due to a bias in AAE retrieval (see major comment 2).

(II) Author's response.

We agree that there are differences, but there is broad consistency, as well. This is more clear in the revised Figure 6, where Shinozuka et al. (2009)'s grey lines (based on the same Russell et al. (2010)'s data) reveal the strong dependence on SSA. This was less clearly indicated by Russell et al. (2010)'s black line.

(I) Comment from Referee:

Section 5.1: Comparison with Saleh et al. is not apples-to-apples. Saleh et al. reports the wavelength-dependence of the imaginary part of the refractive index of the OA only, while this study reports AAE (wavelength-dependence of the absorption coefficient) of the total aerosol (including BC).

(II) Author's response.

The referee is correct for mentioning this issue, which we addressed by previous comments as well. We revised the manuscript accordingly.

(III) Changes in manuscript.

(*) Figure 6 was revised to show that Saleh et al. (2014)'s and Lu et al.(2015)'s curves represent AAE_{OA} .

(*) Sect.5.1 was revised to point out that *we compare, in Fig.6c, different AAE values. In our work, AAE values are due to the bulk dust-free aerosol, thus depending on both BC and OA ($AAE_{BC,OA}$). AAE values of Saleh et al. (2014) and Lu et al. (2015) (AAE_{OA}) come from the wavelength-dependence of OA alone (w_{OA}), excluding contributions from BC (AAE_{OA} values are calculated from w_{OA} based on the relation $AAE = w + 1$, valid for small particles in the visible range). The comparison in Fig.6c is thus intended to compare patterns only, not absolute values.*

(*) The Supplementary Figure 2 was added to show AAE_{BC} together with $AAE_{BC,OA}$, in the AAE vs BC-to-OA plot. We mentioned that *this figure is intended to indicate wavelength dependence of OA absorption, and to suggest possible AAE_{OA} patterns, increasing with decreasing BC-to-OA, similarly to what observed by Saleh et al. (2014) and Lu et al. (2015).*

(I) Comment from Referee:

Section 5.1: The finding that AAE in this study is twice that in Saleh et al. and Lu et al. is most probably not accurate due to overestimation of AAE in this study (see major comment 2).

(II) Author's response.

We agree, and revised Sect.5.1 of the manuscript to mention that *the AAE of this secondary "brown" aerosol would probably be higher than that of the fresh biomass burning OA it likely derives from* (not "twice that", but "higher than that").

(I) Comment from Referee:

Terminology: the authors go back and forth between BrC, brown, and "brown". Please be consistent.

(II) Author's response.

As previously mentioned, *"brown" aerosol does not necessarily equate to brown carbon*. In the revised manuscript, we stressed this and used the *"brown" aerosol* notation everywhere to indicate this aerosol type. BrC was substituted by brown carbon.

2 Referee 2

(I) Comment from Referee:

The concept of measurement uncertainty has not been addressed at all in the manuscript. This needs to be added throughout - especially for the measurements that are central to the analyses: AAE and OA/BC ratio (or BC-to-OA ratio, as in Fig. 4). Similarly, the QA/QC procedures and standards need to be discussed and defended. E.g., all data with $\sigma_a < 1 \text{ Mm}^{-1}$ and $\sigma_s < 10 \text{ Mm}^{-1}$ were removed : why were these the limits imposed? How much data were discarded?

(II)(III) Author's response and Changes in manuscript.

We revised the manuscript to address: (i) uncertainties of optical variables in Sect.2.2; (ii) uncertainty of OA in Sect.2.3; (iii) uncertainty of BC in Sect.3.1; (iv) the resulting uncertainties in the AAE vs BC-to-OA relation in Sect.4.1 (Figure 4 was revised); (v) QA/QC procedures and standards in Sect.2. We referenced previous papers in literature these uncertainties were based on. This is detailed below:

(i) *The uncertainty of the scattering coefficient $\frac{\delta(\sigma_s)}{\sigma_s} = 0.02$, and that of the absorption coefficient $\frac{\delta(\sigma_a)}{\sigma_a} = 0.2$.*

(ii) *The uncertainty of the AMS-derived OA $\frac{\delta(OA)}{OA} = 0.2$.*

(iii) *The uncertainty of BC was calculated by propagating $\frac{\delta(\sigma_a)}{\sigma_a}$, together with the uncertainty deriving from the AAE_{BC} attribution method used to calculate BC. In this method, we set AAE_{BC} = 1.1, and $\frac{\delta(AAE_{BC})}{AAE_{BC}} = 0.22$.*

(iv) *Uncertainties of AAE and BC-to-OA were calculated propagating these values. Figure 4 of the manuscript was revised to include these uncertainties.*

(v) *We mentioned that outlier/low values can significantly influence data statistics. We hence checked carefully values of: (i) $\sigma_a < 1 \text{ Mm}^{-1}$ and $> 50 \text{ Mm}^{-1}$, as PSAP sensitivity $< 1 \text{ Mm}^{-1}$ in the measurement range $0-50 \text{ Mm}^{-1}$; (ii) $\sigma_s < 10 \text{ Mm}^{-1}$ and $> 1000 \text{ Mm}^{-1}$, as nephelometer lower detectable limit = 0.3 Mm^{-1} , with calibration tolerance of $\pm 4 \text{ Mm}^{-1}$, in the measurement range $0-2000 \text{ Mm}^{-1}$. These values are set by instrument manufacturers. A few data (124 records having $\sigma_a < 1 \text{ Mm}^{-1}$, less than 20 records with $\sigma_s < 10 \text{ Mm}^{-1}$, and some points with $\sigma_s > 700 \text{ Mm}^{-1}$) were discarded, as they were considered dubious values, comparing to data variability during the field (illustrated in Supplementary Figure 1).*

(I) Comment from Referee:

In Section 3, what is meant by "The dataset consisted of 11211 records (5764 in fall, and 5447 in winter), including 2551 records (covering 40 days of measurements) with no missing value, and 1087 records (150 in fall, and 937 in winter) of cleaned data after data analysis."?

Does this mean only 10% of the measurements were ultimately included in this analysis?

(II)(III) Author's response and Changes in manuscript.

The referee is right for noting that there was an error. Text was corrected as it follows:

Dataset consisted of 3211 records (1764 in fall, and 1447 in winter). The statistical analysis was done on a subset of these data with no empty field (2551 records, covering 40 days of measurements). These data were then cleaned, and a final dataset of 1487 records (550 in fall, and 937 in winter) was ultimately included in the statistical analysis. The longer dataset was, however, used in the analysis to evaluate single cases (e.g., the case-study).

(I) Comment from Referee: Section 3.2 : what constituted an acceptable merge of the SMPS and APS size distributions? What was considered unacceptable? How many measurements were eliminated using the smoothing procedure and visual inspection?

(II)(III) Author's response and Changes in manuscript.

The referee correctly mentions an issue that was addressed in the revised version (Sect.3.2, P5L24-25).

$PNSD_{fitted}$ replaced $PNSD_{APS}$ and $PNSD_{SMPS}$ when their relative difference (d_r , Eq.1):

$$d_r = \frac{|PNSD_{SMPS} - PNSD_{APS}|}{\max[PNSD_{SMPS}, PNSD_{APS}]} \quad (1)$$

was larger than 0.1 cm^{-3} . This procedure was considered acceptable if: (i) the minimum mean squared error between $PNSD_{fitted}$ and $PNSD_{APS}$ was less than 1%; (ii) correlation coefficients between $PNSD_{fitted}$ and $PNSD_{SMPS}$, and between $PNSD_{fitted}$ and $PNSD_{APS}$ were larger than 0.8. A number of 98 records did not verify these conditions, and were checked by visual inspection: 94 of them were discarded, and 4 accepted.

(I) Comment from Referee:

Section 4.1 and Figures 2-4: discussion is needed to explain the physical meaning of the PC score and the factor loading numbers.

(II) Author's response.

We agree with the referee, and added this in the revised manuscript.

(III) Changes in manuscript.

The following text was added to sect.4.1:

Coefficients of PC_k represent the relative weight (in terms of correlation) of original variables (i.e., time series of $dN/d\log(d_p)$) in PC_k . Factor loadings of PC_k represent these coefficients scaled by the variance explained by PC_k (α_k). Loadings of PC_k thus represent the relative weight of the $dN/d\log(d_p)$ variables in PC_k re-scaled by α_k . Factor scores of PC_k are the transformed variables corresponding to a particular data point in the $dN/d\log(d_p)$ time series. Factor scores thus represent PC_k values corresponding to each particular data point of the $dN/d\log(d_p)$ time series.

(I) Comment from Referee: **Section 4.1 : what does the following sentence mean? "BC mass concentration was assumed to increase mostly with increasing concentration of larger BC particles"? Section 4.1 ? what does the following sentence mean? "Higher fBC values coupled to lower BC mass concentration were, therefore, interpreted as indicators of ultrafine BC particles, and vice versa."**

(II)(III) Author's response and Changes in manuscript.

Both referees (and editor, as well) indicated that this sentence is both unclear and not necessary. To avoid unnecessary text, we decided to delete it (P6L23-28).

(I) Comment from Referee:

Figure 1: it is not clear why the present results from the Po Valley are compared to results from Leipzig made 7-8 years ago?

(II) Author's response.

We revised the manuscript (Sect.4.1) to clarify that: (1) this comparison aims at reinforcing the interpretation that the aerosol type represented by PC_3 is the droplet mode aerosol; and (2) the correlation found between the droplet mode aerosol and the "brown" aerosol demonstrates that the "brown" aerosol is secondary in origin (the droplet mode is secondary in origin), and gives insights into its likely formation process.

(III) Changes in manuscript.

We modified Sect. 4.1 to mention that to our knowledge, results from Leipzig are the only work in literature showing a similar aerosol principal component to compare with. The statistical methodology of the two works is the same, but datasets are very different, in time and space. Results from Leipzig were based on five different statistical analysis based on different datasets (two year data at eight concurrent measurement sites were available to create these five different dataset to be analysed). Results were correlated to meteorological and air quality data. Our work here was based on a shorter time period, and one measurement site. We do believe that results from Leipzig are statistically strong. These identified clearly the PC representing the droplet mode aerosol, which

310 shows *broad similarities with PC3* obtained in our work. *This allows to deduce with a reasonable statistical accuracy that PC3 does represent the droplet mode aerosol.*

(I) Comment from Referee:

The authors have missed some other relevant work that also shows associations between ambient SOA and BrC - see for example X. Zhang et al. (2011; 2013).

315 (II) Author's response.

The referee is right for mentioning that these are important works, both supporting our findings. In fact, we referenced the work by Zhang et al. (2013) in the former manuscript (P2L12, P10L13-15). In the revised manuscript, we referenced these works more explicitly.

(III) Changes in manuscript.

320 (*) In Sect.1 (P2L12-13), we indicated that *secondary organic aerosol (SOA) formed in the atmosphere contributes to the light absorbing carbon, as well (Moise et al., 2015), but only a few works have analysed secondary brown carbon associated to SOA (Zhang et al., 2013, 2011), and Saleh et al.(2013).*

325 (*) In Sect.5.3 (P10L13-15), we mentioned that *the composition found for this "brown" aerosol (high OA, nitrates being a likely component), its formation process (involving aqueous phase reactions), and AAEs values, are all coherent with previous studies, which showed increased light absorption towards UV for SOA particles (Jacobson, 1999; Lee et al., 2013; Song et al., 2013; Zhang et al., 2013; Powelson et al., 2014; Lin et al., 2014; Laskin et al., 2015), and sources, composition, and AAE of light-absorbing soluble organic aerosol in urban areas (Zhang et al., 2013, 2011) .*

330 (I) Comment from Referee:

Section 5.2 and Figure 7: although the "paradigm" discussed here may have been developed in a prior paper, it is not something I think most readers will be familiar with (this reviewer was not). Provide the necessary explanation and context to interpret the present results.

(II) Author's response.

335 We agree with the comment. In the revised manuscript, we added in Sect.5.2: (1) the context (including references to previous relevant works which have analysed the topic); (2) additional explanations to interpret results (including the revised Figure 7), and (3) a Table summarising these results (in particular, k_{530} , which is compared to relevant values of bulk aged OA in literature).

(III) Changes in manuscript.

340 (*) We indicated that *cluster analysis of aerosol spectral optical properties is becoming more and more used to infer information on aerosol type from optical data. We mentioned that Costabile et al. (2013) assessed spectral optical properties of key aerosol populations through Mie theory: soot, biomass burning, two types of organics, dust and marine particles were simulated through a sectional approach where each of these aerosol types was given a monomodal PNSD and a set*
345 *of three refractive indices (RIs) in the visible range. Relevant Angstrom Exponents of extinction, scattering, and absorption (EAE, SAE, AAE), SSA and its spectral variation (dSSA) were calculated. It was proved that these aerosol types separately cluster within a "paradigm" where SAE is on the y-axis, dSSA times AAE is on the x-axis, and SSA is on the z-axis.*

350 (*) We indicated that *experimental data of the "brown" aerosol do cluster in this paradigm (Fig. 7), and that the cluster of "brown" aerosol data is separated from all other simulated aerosol types, except that named "large organics". Data of "large organics" and "brown" aerosol do overlap, indicating that they may represent the same aerosol type. In fact, microphysical properties of the aerosol type named "large organics" were simulated to be same as those of the droplet mode aerosol (i.e., PNSD peaking in the "large" accumulation mode, 300-800 nm size range). Spectral optical prop-*
355 *erties of this "large organics" aerosol type were simulated by RIs of spectrally absorbing organic material in the visible region: these RIs, given the broad similarities in Fig.7, can be assumed to be those of the "brown" aerosol.*

(*) We added Table 1 summarizing these results, and pointed that *this comparison ultimately allows to infer spectral optical properties of "brown" aerosol* (in particular, k_{530} , compared to relevant values recently reviewed by Lu et al. (2015)).

(I) Comment from Referee:

- Section 5.2, lines 28-34: perhaps this is in line with the above comment, but I was completely confused by this entire passage.

(II) Author's response.

Text was changed (see previous comment).

(I) Comment from Referee:

In my opinion, Figure 8 does not much at all to the paper ? I would recommend removing it.

(II) Author's response.

We agree with the referee that this figure is not needed. However, it may be useful to connect results from different aerosol communities. As well, it reinforce findings. We would therefore prefer to keep it.

(I) Comment from Referee:

Section 6: the findings do not "prove" the formation of BrC in the atmosphere.

(II) Author's response.

We agree with the referee, and revised the text (P6L22-23) to mention that *findings show that there is "brown" aerosol in the atmosphere.*

(I) Comment from Referee:

Pg. 7, line 21-22: "The dependence on the nitrate mass fraction (f_{NO3} , Fig.3d) is not obvious, as high AAE values and droplet mode scores are observed for both $f_{NO3} < 0.05$ and $f_{NO3} > 0.25$." This does not seem consistent with the discussion of nitrate's importance in the abstract or in Section 6.

(II) Author's response.

The referee is right and we modified text accordingly, indicating (P1L4-5), that *findings show that "brown" aerosol... contains large concentrations of organic aerosol (OA) in droplet mode particles and that Nitrate is an additional likely component.*

3 Figures and Table changes in manuscript.

We added the following table to summarize spectral optical properties of brown aerosol, and improve clarity of Par. 5.2:

Table 1. Spectral optical properties of the "brown" aerosol in the visible range: AAE, SSA, and SAE (expressed as mean \pm standard deviation and variation range [minimum- maximum value]), and real and imaginary part (k_λ) of the complex refractive index (RI [λ]).

AAE _{467–660}	SSA ₅₃₀	SAE _{467–660}	real part	RI _{λ} k_λ	[λ]
			1.460	$1.2 \cdot 10^{-2}$	[467nm]
3.5 \pm 0.8 [2.5-6]	0.97 \pm 0.01 [0.92-0.99]	0.8 \pm 0.3 [0-2]	1.454	$8 \cdot 10^{-3}$	[530nm]
			1.512	$7.5 \cdot 10^{-3}$	[660nm]

Figure 4 was revised to include relevant uncertainties (not shown before):

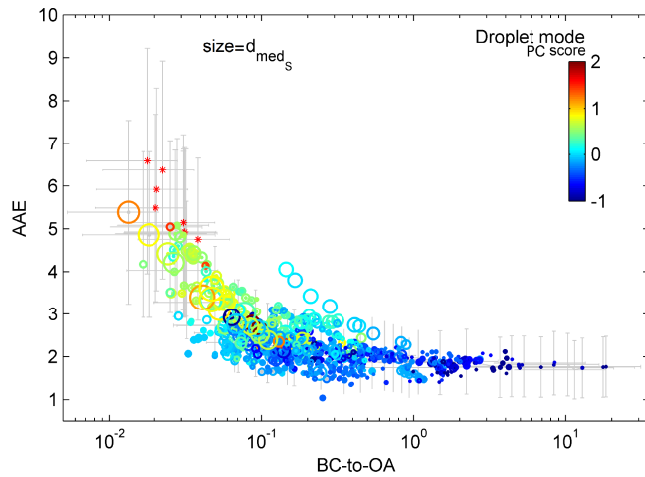


Figure 1. Revised Figure 4 of the manuscript. *Relation between "brown" aerosol and Black Carbon (BC) to Organic Aerosol (OA) ratio (BC-to-OA). Absorption Angstrom Exponent at 467-660 nm (AAE) is plotted against BC-to-OA. Data color is the score of the droplet mode PC extracted by the statistical analysis. Data size is the median diameter of the particle surface size distribution ($d_{med(S)}$). Data indicated by "*" show case-study values illustrated in Fig. 5. Grey bars indicate measurement uncertainty (Sect.2, and 3.1).*

390 Figure 6 was revised to include Shinozuka et al. (2009) and Lu et al. (2015) data:

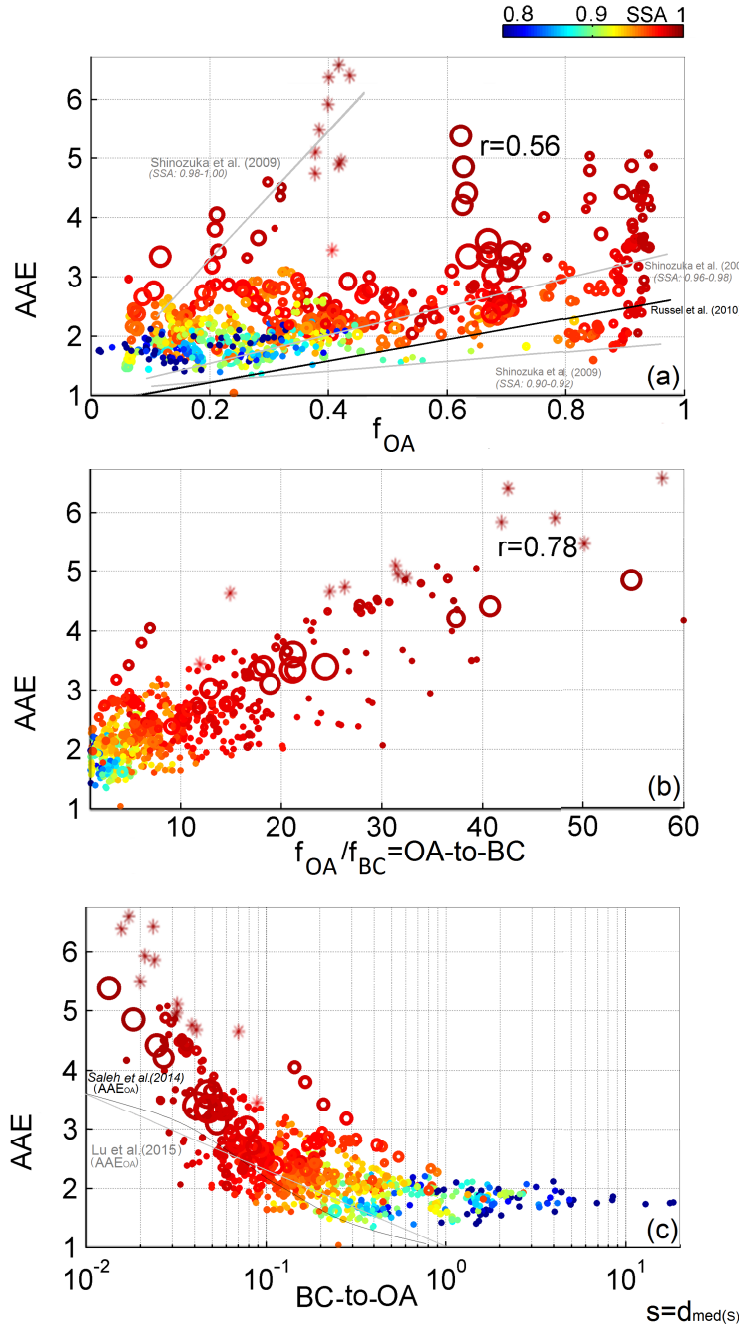


Figure 2. Revised Figure 6 of the manuscript. *Dependence of Absorption Angstrom Exponent at 467-660 nm (AAE) on (a) organic aerosol mass fraction (f_{OA}), (b) Organic Aerosol (OA) to Black Carbon (BC) ratio (OA-to-BC), and (c) BC-to-OA ratio. Data color is Single Scattering Albedo at 530 nm. Data size is median diameter of particle surface size distributions ($d_{med,s}$, ranging from 50 to 300 nm). Data indicated by "*" show case study values illustrated in Fig. 5. Relevant Pearson's correlation coefficients (r) are indicated. For comparison, we show previous results: (a) by Russell et al. (2010) (black line) and ? (grey lines, for the SSA bins of 0.90-0.92, 0.96-0.98 and 0.98-1.00); (c) by ? (black line), and Lu et al. (2015) (grey line). Note that AAE includes contributions from both BC and OA, whereas in panel (c), Lu et al. (2015) ?'s results refer to AAE_{OA} only.*

Figure 7 was revised to improve clarity. The rev.Fig.7 includes panel a only, whereas panel b of the former Fig.7 was added in the Supplementary material:

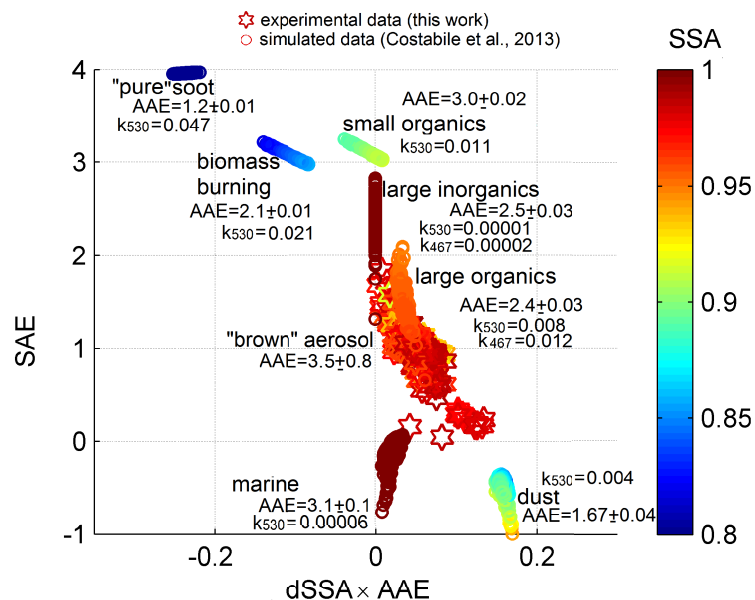


Figure 3. Revised Figure 7 of the manuscript (including panel a of the former Figure 7 only).

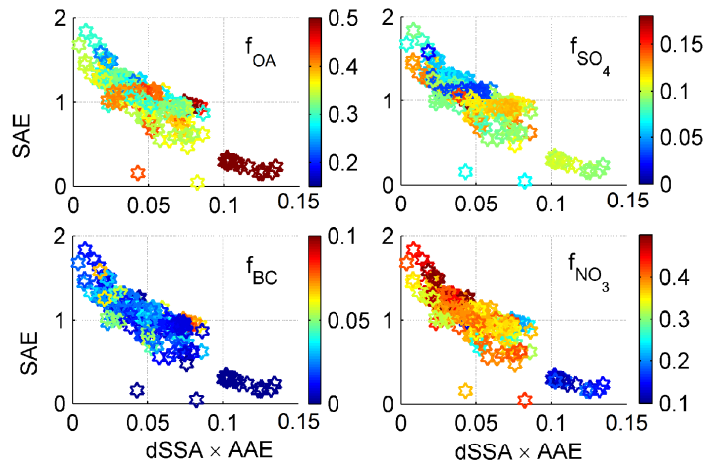


Figure 4. Supplementary Figure, showing panel b of the former Figure 7.

The following figure was added in the supplementary material to show relative proportions of BC and OA in the AAE against BC-to-OA relation:

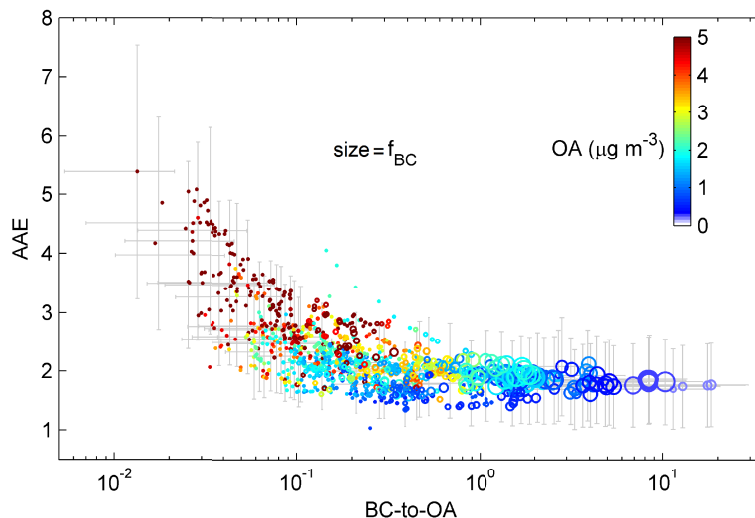


Figure 5. Supplementary Figure. *Relative proportions of BC and OA in the AAE vs BC-to-OA relation. BC-to-OA ratio (x-axis) against Absorption Angstrom Exponent (y-axis). Data points are sized by BC mass fraction (f_{BC}), and colored by organic aerosol mass concentration (OA). Vertical and horizontal bars show uncertainties (see Sect.3.1)*

395 The following figure was added in the supplementary material to show $AAR_{BC,OA}$ against AAE_{BC} :

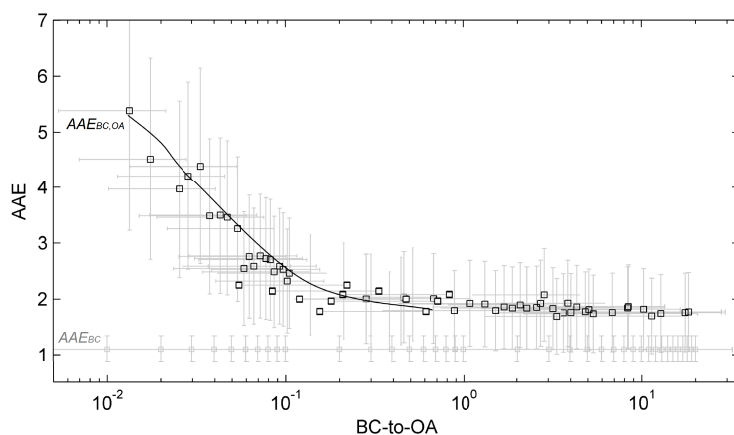


Figure 6. Supplementary Figure. *Dependence of the Absorption Angstrom Exponent (AAE) due to organic aerosol (OA) from the BC-to-OA ratio. The AAE due to BC and OA ($AAE_{BC,OA}$) of the dust-free bulk AAE is indicated by black squares. (A subset of data is indicated with uncertainty-bars (grey lines), the interpolating curve of the whole dataset being indicated by the black curve). AAE_{BC} used to derive BC is also indicated (grey squares).*

The following figure was added in the supplementary material to show loadings and scores calculated by PCA of the four PCs of PNSD:

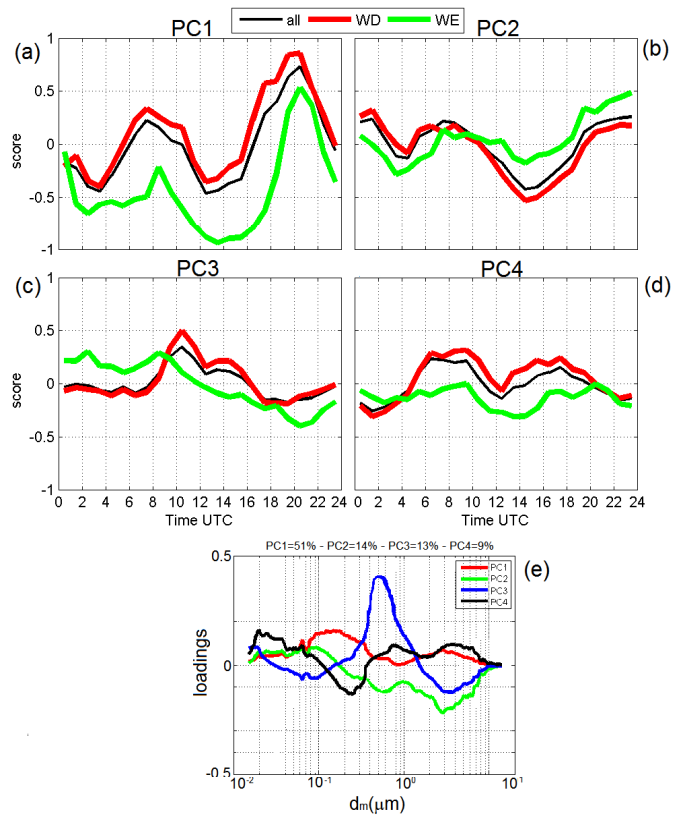


Figure 7. Supplementary Figure. *Principal components (PC1-PC4) of the Particle Number Size Distributions: (a-d) weekly diurnal cycles of scores (red, Week Day; green, Week End; black, all data), and (e) loadings.*

The following figure was added in the supplementary material to show extensive spectral optical properties during the two field campaigns:

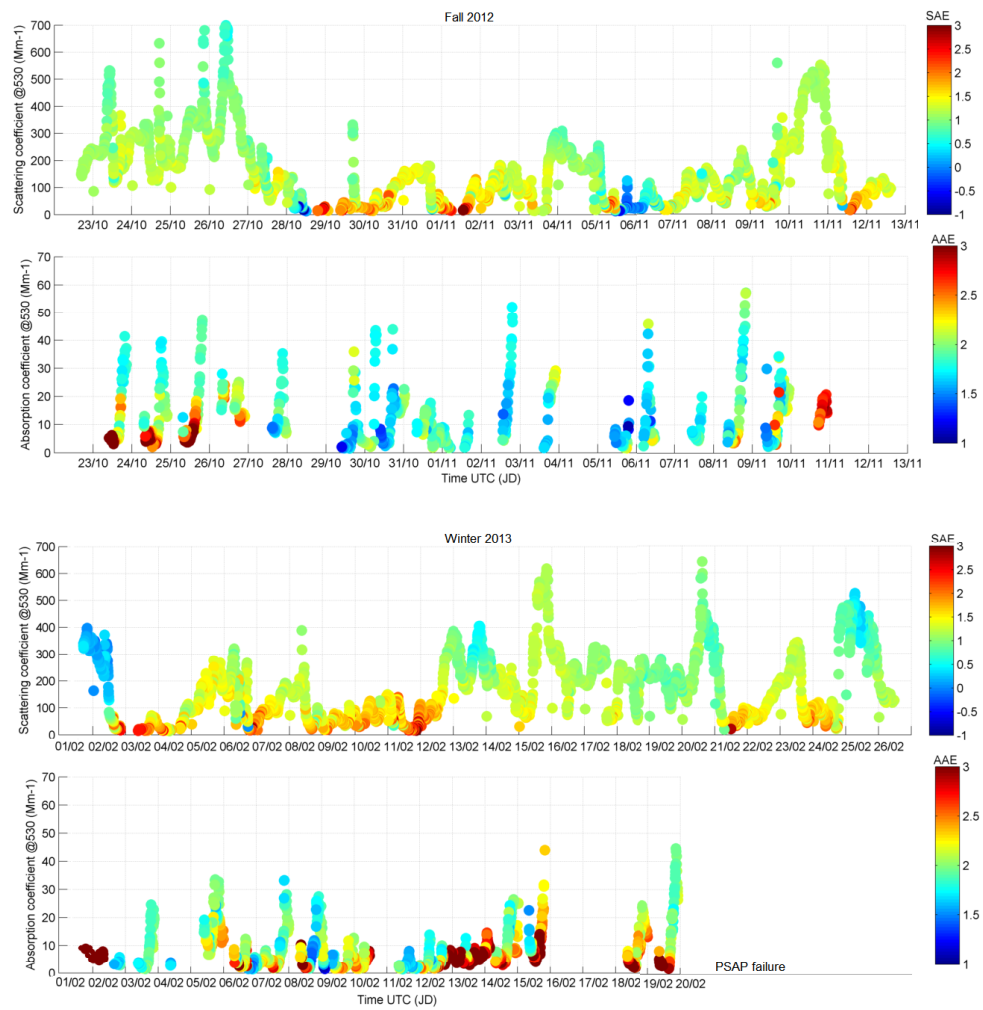


Figure 8. Supplementary Figure. *Spectral optical properties during field campaigns: y-axis shows data of scattering and absorption coefficients, colored by the Scattering Angstrom Exponent (SAE), and Absorption Angstrom Exponent (AAE), respectively.*

400 References

- Lack, D.A., Cappa, C.D., Covert, D.S., Baynard, T., Massoli, P., Sierau, B., Bates, T.S., Quinn, P.K., Lovejoy, E.R. and Ravishankara, A.R.: Bias in filter-based aerosol light absorption measurements due to organic aerosol loading: Evidence from ambient measurements. *Aerosol Science and Technology*, 42(12), pp.1033-1041, 2008.
- 405 Lack, D. A. and Langridge, J. M.: On the attribution of black and brown carbon light absorption using the Ångström exponent, *Atmos. Chem. Phys.*, 13, 10535-10543, doi:10.5194/acp-13-10535-2013, 2013.
- Pöschl, U.: Aerosol particle analysis: challenges and progress. *Anal. Bioanal. chem.*, 375.1, 30-32, DOI 10.1007/s00216-002-1611-5, 2003.
- Zhang, X., Y.-H. Lin, J. D. Surratt, and R. J. Weber: Sources, composition and absorption Ångström exponent of
410 light-absorbing organic components in aerosol extracts from the Los Angeles Basin, *Environ. Sci. Technol.*, 47(8), 3685-3693, 2013.
- Zhang, X., Lin, Y. H., Surratt, J. D., Zotter, P., Prévôt, A. S., Weber, R. J.: Light-absorbing soluble organic aerosol in Los Angeles and Atlanta: A contrast in secondary organic aerosol. *Geophys. Res. Lett.*, 38(21), 2011.

Characteristics of ~~an aged organic~~ "brown" aerosol in the urban Po Valley atmosphere

F. Costabile¹, S. Gilardoni², F. Barnaba¹, A. Di Ianni¹, L. Di Liberto¹, D. Dionisi¹, M. Manigrasso³, M. Paglione², V. Poluzzi⁴, M. Rinaldi², M.C. Facchini², and G. P. Gobbi¹

¹Institute for Atmospheric Sciences and Climate (ISAC), National Research Council (CNR), Rome, Italy

²Institute for Atmospheric Sciences and Climate (ISAC), National Research Council (CNR), Bologna, Italy

³INAIL, Rome, Italy

⁴ARPA ER, Bologna, Italy

Correspondence to: F. Costabile (f.costabile@isac.cnr.it)

Abstract. We ~~characterize the atmospheric~~ characterized the nondust aerosol having the strongest spectral ~~dependence~~ dependance of light absorption (as indicated by the Absorption ~~Angstrom~~ Ångström Exponent, AAE) at visible wavelengths in the urban ~~Po Valley~~ ambient atmosphere of the Po Valley (Bologna). ~~We defined "brown" this bulk aerosol with brown color (it does not necessarily equate to brown carbon).~~ In situ ground measurements of aerosol spectral optical properties, PM₁ chemical composition (HR-ToF-AMS), and coarse and fine size distributions, were carried out in Bologna, and data statistically analysed. ~~Findings prove that a "brown" aerosol (AAE from 2.5 to 6) in the ambient atmosphere is composed by "droplet" mode particles enriched in aged organic aerosol (OA) and nitrate. We provide a comprehensive physico-chemical characterisation of this brown aerosol, including its spectral optical signature, and possible sources.~~ Findings prove that "brown" aerosol is a secondary aerosol with AAE values from 2.5 to 6, containing large concentrations of organic aerosol (OA) in the larger accumulation mode particles previously referred to as droplet mode particles. Nitrate is an additional likely component. Its spectral optical signature, and possible sources, are investigated. To our knowledge, no previous work has considered these issues in the ambient atmosphere. We compared to literature to put findings in a broader perspective. There is consistency with recent "diluted" urban observations (airborne, and AERONET), and combustion chamber observations. Our study adds to these previous ones that the high AAE values featuring the "brown" aerosol depend on the OA to Black Carbon (BC) ratio more than on OA, and that the link between AAE and OA-to-BC (already observed for freshly emitted primary aerosols from biomass burning) does exist in the ambient atmosphere for this aged "brown" aerosol, as well. The comparison with studies on the composition evolution of OA in the atmosphere strengthens the result

that this "brown" aerosol ~~is an aged OA, and provides experimental evidence for the aged "brown" OA formation in the ambient atmosphere~~contains aged OA, and give insights into aged brown OA formation processes. Findings will have important atmospheric implications for modeling studies, and remote sensing observations, as regards ~~the~~ parametrization and identification of ~~Brown~~brown OA, and ~~Brown Carbon~~brown carbon in the atmosphere.

1 Introduction

Aerosol has an important role in the Earth's climate with both direct and indirect effects; beside that, it affects air quality and atmospheric chemistry. At present, our understanding of the light-absorbing aerosol types is very incomplete (see reviews by Laskin et al., 2015; Moise et al., 2015). An important absorber of solar radiation in the visible region is the atmospheric carbonaceous aerosol (IPCC 2013). ~~Visible-light absorbing properties of this aerosol type vary~~In the classification of its components proposed by poschl2003, visible-light absorbing properties were varied between two extremes. On one side, there is Black Carbon (BC), refractory material that strongly absorbs light over a broad spectral range. On the other side, there is the colourless Organic Carbon (OC), non-refractory material, with no absorption or little absorption in the UV spectral range. ~~Between these extremes~~There is a gradual decrease of thermochemical refractiveness and specific optical absorption going from BC graphite-like structures to non-refractive and colorless OC. Also, there is a gradual decrease in the volatility from BC (the lowest volatility), to colorless non-refractory volatile OC (the highest volatility). A broad range of coloured (~~moderately volatile~~) organic compounds~~that organic compounds, with volatility in between these two extremes~~, have recently emerged in the scientific literature for their possible role in the Earth's climate. The term "brown carbon" (BrC) has emerged to describe this aerosol having an absorption spectrum smoothly increasing from the vis to the near-UV wavelengths, with a strong wavelength dependence of the light absorption coefficient ($\lambda^{-2} - \lambda^{-6}$) (Andreae and Gelencsér, 2006; Moosmüller et al., 2011; Bond et al., 2013; Laskin et al., 2015; Moise et al., 2015). In fact, BrC lacks a formal analytical definition (Bond et al., 2013). In this study, we will refer to a "brown" aerosol to indicate an aerosol type with high values (2-6) of the Absorption Ångström Exponent (AAE), a parameter describing the wavelength (λ) dependent absorption coefficient (σ_a) of light by aerosol, written as:

$$AAE(\lambda) = -\frac{d \ln(\sigma_a)}{d \ln(\lambda)}.$$

What is known about the BrC aerosol is that it is an organic matter having both primary and secondary sources (Laskin et al., 2015). Primary BrC can be emitted together with BC from low-temperature combustion processes, like wood combustion (Andreae and Gelencsér, 2006). Secondary organic aerosol (SOA) formed in the atmosphere contributes to the light absorbing carbon, as

~~(Moise et al., 2015). Little is known about sources of the secondary BrC (Moise et al., 2015, and references therein), but only a few works have analysed the secondary brown carbon associated to SOA (Saleh et al., 2013; Zhang et al., 2013)(Saleh et al~~

Numerous evidences indicate increased absorption towards UV for aerosol particles having high nitrate (e.g., Zhang et al., 2013; Jacobson, 1999) and sulfate contents (Powelson et al., 2014; Lin et al., 2014; Lee et al., 2013; Song et al., 2013). Lin et al. (2014) reported the formation of light-absorbing SOA constituents from reactive uptake of isoprene epoxydiols onto preexisting acidified sulfate seed aerosol as a potential source of secondary BrC under tropospheric conditions. Powelson et al. (2014) discussed the BrC formation by aqueous-phase carbonyl compound reactions with amines and ammonium sulfate. Lee et al. (2013) studied the likely and unknown effect of sulfate on the formation of light absorbing materials and organo-nitrogen via aqueous glyoxal chemistry in aerosol particles. Song et al. (2013) observed significant light absorption at 355 and 405 nm for the SOA formed from an α -pinene + O₃ + NO₃ system only in the presence of highly acidic sulfate seed aerosols under dry conditions. Several studies demonstrated the importance of ammonium, both as a catalyst and as a reactant, in the formation of light-absorbing products (Laskin et al., 2015; Powelson et al., 2014). SOA formation can occur both in the gas and condensed phase. Recently, an efficient SOA production has been recognised in cloud/fog drops and water containing aerosol: water soluble products of gas phase photochemical reactions may dissolve into an aerosol aqueous phase and form SOA through further oxidation, this SOA being referred to "aqSOA" (Ervens et al., 2011; Laskin et al., 2015). AqSOA formation impacts total SOA mass, and aerosol size distributions by adding mass to the so-called "droplet mode" (Ervens et al., 2011). Meng and Seinfeld (1994) showed that the aerosol "droplet mode" in urban areas is the result of activation of smaller particles to form fog, followed by aqueous-phase chemistry, and fog evaporation. It was demonstrated that aqSOA formation can affect aerosol optical properties by adding light-absorbing organic material at UV wavelengths (Shapiro et al., 2009; Ervens et al., 2011).

Despite the efforts made, relations between optical properties and chemical composition of organic compounds with spectrally variable light absorption (high AAE) are poorly understood (Laskin et al., 2015). A number of previous works (Shinozuka et al., 2009; Russell et al., 2010; Arola et al., 2011) studied how the organic aerosol (OA) mass fraction (f_{OA}) relates to AAE, and to Single Scattering Albedo (SSA), the ratio of scattering to extinction, a key parameter to understand aerosol warming or cooling effect. Results from in situ measurements on the C-130 aircraft mostly over Central Mexico during MILAGRO (Russell et al., 2010) showed that both Organics and dust increase AAE values. Russell et al. (2010) showed a direct correlation between AAE and f_{OA} , the larger particles (dust) having higher AAE, and the smaller particles (pollution related) having lower AAE. On the basis of the same data, Shinozuka et al (2009) showed that AAE generally increases as f_{OA} or SSA increases. This was explained by the presence of humic like substances (HULIS) and dust, which are colored (high AAE), weak absorbers (high SSA), with high f_{OA} . Very recently, Saleh et al. (2014) burnt a selection of biomasses in a combustion chamber, varying the combustion parameters to obtain a range of BC-to-OA ratios. This ratio, the relative proportions of BC and OA mass, depends on fire characteristics, and determine its colour from black to brown to white as the

ratio decreases (Bellouin, 2014). Their findings link the extent of absorbance to the BC-to-OA ratio
95 for aged and fresh biomass burning aerosols. If confirmed by further studies, this link can be a po-
tentially strong predictive tool for light-absorbing properties of biomass burning aerosols (Bellouin
, 2014; Moise et al., 2015). Following the Saleh et al. (2014)'s idea, Lu et al. (2015) reviewed avail-
able emission measurements of biomass burning and biofuel combustion, and found similar results
indicating that AAE of the bulk OA decreases with the BC-to-OA ratio. They conclude that the ab-
100 sorptive properties of OA from biomass/ biofuel burning depend strongly on burning conditions and
weakly on fuel types and atmospheric processing.

In this study, we characterize the nondust aerosol having the strongest spectral dependance of
light absorption (as indicated by the AAE) at visible wavelengths in the ambient atmosphere. In situ
ground ambient measurements of chemical (HR-ToF-AMS), optical (3- λ nephelometer and PSAP),
105 and micro-physical (SMPS and APS) aerosol properties were taken in Bologna, Po Valley, together
with ancillary observations (including ceilometer retrievals). Major features of the "brown" aerosol
in the ambient urban atmosphere are investigated. We used a global approach where the aerosol type,
as a whole, is linked to the highest AAE values. We investigate sources of this brown aerosol by
relating AAE to primary and secondary aerosol populations extracted through a statistical analysis
110 of size distribution, and mass spectral features. We then characterise physico-chemical properties of
the observed brown aerosol, and illustrate a case-study. Findings are then discussed in comparison
with previous literature works to explore their general validity instead of treating them like results
of a local study.

2 Experimental

115 Optical, chemical, and microphysical aerosol properties were measured, in the framework of the
ARPA ER Supersite project, at the urban background site of Bologna (44 ° 31' 29" lat, 11 ° 20' 27'
lon), in the Po Valley (Italy). Two measurement campaigns lasting one month were taken: October 22
- November 13, 2012 (Fall campaign), and February 1-27, 2013 (Winter campaign). Measurements
performed are detailed below.

2.1 Measurement cabins and sampling lines

Equipment was set up in two different cabins, located side by side. Optical properties and coarse frac-
tion size distributions were measured in the same cabin, all the instruments set-up on the same inlet
system equipped with a PM₁₀ head. External air was pumped in the cabin into a stainless steel tube
(length = 4.0 m) by an external pump ensuring a laminar flow (Reynolds number <2000). The cabin
125 was conditioned at 20-25°C. The difference between air temperature and dew point was enough to
dry sampled air. Chemical properties and fine and ultrafine particle number size distribution were
measured through a separate stainless steel inlet tube equipped with a PM₁ head.

2.2 Optical Measurements

Spectral optical properties in the visible range were measured online with a 5 minute time resolution.

~~The dry aerosol absorption coefficient~~ Dry aerosol absorption coefficients, $\sigma_a(\lambda)$, at three wavelengths ($\lambda = 467, 530, 660$ nm) ~~was~~ were measured by a 3-wavelength particle soot absorption photometer (PSAP, Radiance Research). ~~Raw PSAP data were corrected according to previous work by Bond et al. (1999); Virkkula et al. (2005); Virkkula (2010). The correction procedure requires wavelength resolved, together with dry aerosol~~ scattering coefficients ($\sigma_s(\lambda)$) ~~; which were derived from measurements~~

~~of the dry aerosol $\sigma_s(\lambda)$~~ at 450, 525, and 635 nm, ~~performed~~ by an integrating nephelometer (Ecotech, mod. Aurora 3000). ~~All measurements with~~ Like all filter based methods, PSAP suffers from a

number of measurement artifacts, including an overestimate of absorption if light absorption is also affected by particulate light scattering, and a dependence of measurements on filter transmittance (Tr).

There are in literature correction algorithms developed to overcome these artifacts - Lack et al. (2008); Virkkula (2010); Backman

et al. (1999), and the comprehensive review by Bond et al. (2013). We corrected raw PSAP data after the iterative procedure finally described by Virkkula (2010), where only data with Tr > 0.7 were retained. The wavelength-resolved $\sigma_s(\lambda)$ necessary to correct PSAP raw data were taken from nephelometer data corrected for truncation (Anderson and Ogren (1998), Bond (2001), and Müller et al., 2011). The scattering error after the truncation error correction is $\frac{\delta(\sigma_s)}{\sigma_s} = 0.02$ (Bond et al., 2013).

The uncertainty of $\sigma_a(\lambda)$ ~~←~~ derived from PSAP data after these corrections has been estimated to be $\frac{\delta(\sigma_a)}{\sigma_a} = 0.2$ (Virkkula, 2010; Lack et al., 2008; Bond et al., 1999; Virkkula, 2010; ?) Cappa et al., 2008). These PSAP-derived $\sigma_a(\lambda)$ can be considered an upper limit of the "true" value (Subramanian et al., 2007; Lack et al., 2008).

After all corrections, data were checked (by visual inspection) to find any outlier/low values that could significantly influence data statistics. These values can be due to variability in the measurements or to experimental errors. According to manufacturers: (i) PSAP sensitivity is $< 1 \text{ Mm}^{-1}$, and $\sigma_s(\lambda)$ ~~←~~ measurement range is $0-50 \text{ Mm}^{-1}$; (ii) the lower detectable limit of the nephelometer is 0.3 Mm^{-1} , with calibration tolerance of $\pm 4 \text{ Mm}^{-1}$, and measurement range $0-2000 \text{ Mm}^{-1}$. A few data (124 records having $\sigma_a < 1 \text{ Mm}^{-1}$, less than 20 records with $\sigma_s < 10 \text{ Mm}^{-1}$ ~~were eliminated to~~ reduce possible experimental errors from the dataset, and some points with $\sigma_s > 700 \text{ Mm}^{-1}$) were discarded, as they were considered dubious values (comparing to data variability during the field, illustrated in the Supplementary Fig. 1).

2.3 Chemical Measurements

Chemical composition of atmospheric aerosol particles were characterized online with a High Resolution Time of Flight Aerosol Mass Spectrometer (HR-ToF-AMS, Aerodyne Research Inc., Billerica) (DeCarlo et al., 2006). The HR-ToF-AMS measured the chemical composition of non-refractory PM_1 (nr- PM_1), i.e sulfate, nitrate, ammonium, chloride, and organic aerosol. The instrument alter-

nated acquisition in V-mode (higher sensitivity and lower mass spectral resolution), and W mode (lower sensitivity and higher mass spectral resolution) every 2.5 minutes. Quantitative information discussed here corresponds to the data collected in V mode. While operating in the V mode, the instrument measures particle size distribution based on their time of flight (Jimenez et al., 2003). HR-ToF-AMS data were analyzed using SQUIRRELL v1.51 and PIKA v1.10 software (D. Sueper, University of Colorado, Boulder, CO, USA) within Igor Pro 6.2.1 (WaveMetrics, Lake Oswego, OR). Collection efficiency was calculated according to Middlebrook et al. (2012) based on aerosol chemical composition, and relative humidity. Data validation was performed by comparison with offline measurements of sulfate, ammonium, and nitrate concentrations in PM₁ aerosol samples. The HR-ToF-AMS aerosol sample line was dried below 40% RH with a Nafion drier. The uncertainty of the AMS-derived OA was assumed to be $\frac{\delta(OA)}{OA} = 0.2$ according to Quinn (2008).

2.4 Particle Number Size distributions

Particle number size distributions (PNSDs) were measured by combining a commercial Scanning Mobility Particle Sizer (SMPS, TSI mod. 3080 with Long-DMA, TSI mod. 3081, equipped with a water-based Condensation Particle Counter, CPC, TSI mod. 3787), and a commercial Aerodynamic Particle Sizer (APS, TSI). Particles from 14 nm to 750 nm of mobility diameter were sized and counted by the SMPS; particles from 0.5 to 20 μm of aerodynamic diameter were sized and counted by the APS (the procedure to fit the two PNSDs is described in the Sect.3.2). SMPS data were corrected for penetration errors through the sampling line, penetration efficiency due to diffusion losses (calculated according to Hinds (1999)) being higher than 98% for particles bigger than 14 nm. An impactor (nozzle of 0.457 μm) was used to remove larger particles.

3 Data analysis

Data measured by all the instruments were merged in a single dataset of 5 minute resolution. ~~The dataset consisted of 11211 records (5764 in fall, and 5447 in winter), including.~~ Dataset consisted of 3211 records (1764 in fall, and 1447 in winter). ~~The statistical analysis was done on a subset of these data with no empty field (2551 records), covering 40 days of measurements) with no missing value, and 1087 records (+50).~~ These data were then cleaned, and a final dataset of 1487 records (550 in fall, and 937 in winter) of cleaned data after data analysis, was ultimately included in the statistical analysis. The longer dataset was, however, used in the analysis to evaluate single cases (e.g., the case-study).

3.1 Inference of the optical Black Carbon mass concentration

~~A~~ The wavelength (λ) dependent BC absorption coefficient ($\sigma_{aBC}(\lambda)$), and equivalent BC mass concentration, were calculated using the AAE_{BC} attribution method. The measured absorption coefficient at 660 nm ($\sigma_a(660)$) was used to derive $\sigma_{aBC}(530)$, and then the BC mass concentration,

assuming: (i) ~~a known value of $AAE_{530-660}$ of σ_{aBC} to be 1~~ $_{BC}$ at 530-660 nm (see below), and
(ii) BC Mass Absorption Efficiency at 530 nm to be $10 \text{ m}^2 \text{ g}^{-1}$ (~~see Costabile et al. (2015) for more details~~), as indicated by PSAP manufacturer). In literature, $AAE_{BC}=1$ is a commonly used value for externally mixed BC; internally mixed BC is commonly assumed to have the same $AAE_{BC}=1$.
200 In fact, AAE_{BC} for externally mixed BC has been predicted to be 1 for particles with diameter < 50 nm (e.g., Bergstrom et al., 2002; Moosmüller et al., 2011), but can range from 0.8 to 1.1 for particle diameters of 50-200 nm (Gyawali et al., 2009). For ambient particles, which can be internally or externally mixed, AAE_{BC} for visible wavelengths has often been observed to be larger than 1 (Lack and Langridge, 2013; Shinozuka et al., 2009, and references therein). Theoretical calculations
205 have shown that the AAE_{BC} for internally mixed BC can vary from 0.55 (e.g., Bahadur et al., 2012) to an upper limit of ~ 1.7 (e.g., Lack et al., 2008) depending on particle size, coating, core, wavelengths. Based on these works, we decided to use $AAE_{BC}=1.1$. The uncertainty was set to $\frac{\delta(AAE_{BC})}{AAE_{BC}}=0.22$ (Lack and Langridge, 2013). BC uncertainty ($\delta(BC)$) was derived propagating this $\delta(AAE_{BC})$ together with the uncertainty of PSAP-derived σ_a (see Sect.2.2).

210 We discarded data possibly affected by desert dust (43 records over 5 days of measurements) to ensure that the equivalent BC mass concentration is not affected from contamination by desert dust. ~~Dust presence was~~ Dust-free aerosol conditions were identified based on the ~~information provided by the bulk analysis of~~ aerosol spectral optical properties (Russell et al., 2010). ~~In particular, we fixed threshold on the Scattering Angstrom Exponent (SAE), the AAE, and the~~ increasingly applied to
215 gather information on aerosol type (e.g., Bergstrom et al., 2007; Clarke et al., 2007; Yang et al., 2009; Russell et al., 2010; Gyawali et al., 2012; Lee et al., 2012; Costabile et al., 2013). We followed the methodology proposed by Costabile et al. (2013) (further discussed in Sect.5.2). Accordingly, the aerosol dominated by dust shows this distinctive combination of scattering, and absorption Angstrom Exponents (SAE, AAE), and Single Scattering Albedo (SSA) (~~Costabile et al., 2013~~).
220 spectral variation (dSSA): $SSA_{530} > 0.85$, $SAE_{467-660} < 0.5$, $AAE_{467-660} \sim 2$, $dSSA_{660-467} = 0.05-0.3$. Data points of the time series fulfilling all these conditions together were excluded from the analysis.

3.2 Fitting procedure for the particle number size distribution

Data of particle number size distributions (PNSDs) were measured by two different instruments
225 (SMPS and APS, Sect.2). These data were merged to obtain one PNSD based on particle electrical mobility diameters (d_m) ranging from 14 nm to $14 \mu\text{m}$. PNSDs measured by APS are based on aerodynamic diameters (d_a); these data were converted to PNSDs based on d_m according to Eq.1 (Khlystov et al., 2004; Seinfeld and Pandis, 2006):

$$d_m = \chi \frac{C_c(d_m)}{C_c(d_a)} \frac{d_a}{\left(\frac{\rho_p}{\rho_0 \chi}\right)^{1/2}} \quad (1)$$

230 where χ is the shape factor, $C_c(d_m)$ and $C_c(d_a)$ are the slip correction factors based on d_m and d_a respectively, ρ_p is the particle density, and ρ_0 is the unit density ($1 \text{ g}\cdot\text{cm}^{-3}$). In applying Eq.1 to convert APS data, we assumed: particle diameter (d_p) = d_m ; $C_c(d_m) = 1$ and $C_c(d_a) = 1$ (continuum regime); $\chi = 1$ (spherical particles); ρ_p continuously varying from 1.6 to $2 \text{ g}\cdot\text{cm}^{-3}$.

235 ~~PNSDs-Particle Number Size Distributions, $n_N(\log_{10}d_m) = \frac{dN}{d\log_{10}(d_m)}$, measured by SMPS and APS (PNSD_{SMPS} , PNSD_{APS}) overlap for d_m ranging from 460 nm to 593 nm. The two PNSDs were then fitted by~~ In this size range, PNSD_{SMPS} and PNSD_{APS} were replaced by PNSD_{fitted} . PNSD_{fitted} was assumed to vary according to a power-law function (Junge size distribution) (Khlystov et al., 2004; Seinfeld and Pandis, 2006) , meaning that the lognormal PNSD defined in Eq.??:

$$\underline{n_N(\log_{10}d_m) = \frac{dN}{d\log_{10}(d_m)}},$$

240 ~~is assumed to vary according to Eq.2:~~ (Eq.2):

$$n_N(\log_{10}d_m) = \frac{c}{d_m^\alpha}, \quad (2)$$

where

~~The coefficients c and α are two coefficients. The following iterative procedure was used to correct data when APS lognormal PNSD differed by more than 0.1 cm^{-3} from SMPS lognormal PNSD were~~
 245 ~~calculated by an iterative procedure:~~ (i) ~~the coefficient c is c~~ was randomly initialized from 0 to 1000; (ii) ~~the value of α is~~ was calculated by Eq.2 assuming a value ~~constraining values~~ from 2 to 5 typical of atmospheric aerosol (Seinfeld and Pandis, 2006); (iii) the fitted lognormal PNSD is calculated by Eq.2; (iv) results are constrained by minimizing mean square error between calculated lognormal PNSD and APS lognormal PNSD, and maximising correlations between SMPS lognormal PNSD and
 250 ~~APS lognormal PNSD. Fitted PNSDs were further corrected, as typically found for atmospheric aerosols (Seinfeld and Pandis, 2006). PNSD_{fitted} replaced PNSD_{APS} and PNSD_{SMPS} when their relative difference (d_r , Eq.4):~~

$$\underline{d_r = \frac{|\text{PNSD}_{SMPS} - \text{PNSD}_{APS}|}{\max[\text{PNSD}_{SMPS}, \text{PNSD}_{APS}]}} \quad (3)$$

~~was larger than 0.1 cm^{-3} . This procedure was considered acceptable if: (i) the minimum mean squared error between PNSD_{fitted} and PNSD_{APS} was less than 1%; (ii) correlation coefficients between PNSD_{fitted} and PNSD_{SMPS} , and between PNSD_{fitted} and PNSD_{APS} were larger than 0.8. A number of 98 records did not verify these conditions, and were checked by visual inspection through a smoothing procedure, and suspected cases eliminated: 94 of them were discarded, and 4 accepted.~~ The final dataset contained PNSD data based on d_m from 14.1 to 429.4 nm measured
 260 by the SMPS, from 446.1 to 699 nm generated by the fitting procedure, and from 0.7 to $14 \mu\text{m}$ measured by the APS .

4 Results and discussion

In this section, we first identify a "brown" aerosol (AAE from 2 to 6) by relating AAE to key aerosol populations extracted through a combined statistical analysis of PNSD, and organic aerosol mass spectra. We then characterise physico-chemical properties of the observed "brown" aerosol as regards number and mass size distribution (and relevant modes), and major PM₁ chemical components (BC, organics, nitrate, ammonium, and sulfate), relevant mass fractions, and ratios. A case-study is finally illustrated.

4.1 A "brownBrown" aerosol type: identification and features

Key aerosol types were identified through a statistical approach. PNSD principal components (PCs) were identified by Principal Component Analysis (PCA). PCA was calculated following the findings of a previous long-term study over multiple sites (8 concurrent stations) by Costabile et al. (2009). Four principal components (PC1-PC4) were extracted, explaining 90% of the variance. We interpreted these PCs based on: (i) their statistical properties, i.e. "scores" and "loadings" (loadings indicate correlations between PNSDs and PCs, i.e. the "mode" of the PNSD associated to the PC); (ii) Pearson's correlation coefficients (r) shown in Table 1, between PCs, AAE, and PM₁ mass fractions of BC, organics, nitrate, sulfate, and ammonium (f_{BC} , f_{OA} , f_{NO_3} , f_{SO_4} , f_{NH_4}). The median diameter of the particle surface size distribution ($d_{med(S)}$) in Table 1 is intended to add information on optically relevant aerosol sizes. The coupling of BC mass concentration and f_{BC} in Table 1 is intended to give information on BC particle size. BC mass concentration was assumed to increase mostly with increasing concentration of larger BC particles, as mass depends on volume (BC mass concentration of accumulation mode BC particles is larger than that of soot mode BC particles, all other things being equal). Higher f_{BC} values were assumed to characterize freshly emitted BC particles, as atmospheric ageing increases non-BC particle coating (thus decreasing f_{BC}). Higher f_{BC} values coupled to lower BC mass concentration were, therefore, interpreted as indicators of ultrafine BC particles, and vice versa. The OA to BC ratio (OA-to-BC) in Table 1 is intended to indicate both combustion characteristics (higher for biofuels than for fossil fuel combustion), and aerosol ageing (lower for fresh aerosols) (Saleh et al., 2014; Bond et al., 2013). Correlations to f_{43} and f_{44} (defined as the ratio of the AMS signal at m/z 43 and m/z 44, respectively, to the total organics AMS signal) in Table 1 are intended to add information on the oxidised OA. The higher the f_{44} , the more oxidised the OA; the higher the f_{44}/f_{43} ratio, the lower the volatility of this oxidised OA (Ng et al., 2010, 2011; Moise et al., 2015).

Statistical properties used to interpret PC are "scores" and "loadings". PCs retained in the analysis were arranged in decreasing order of variance explained (λ_k , called eigenvalue of PC _{k}), PC1 being the component explaining the largest λ_k . The k^{th} eigenvector is composed of scalar coefficients describing the new PC _{k} as a linear combination of the original variables (the original variables are the

time series of $dN/d\log(d_p)$). Coefficient of PC_k represent the relative weight (in terms of correlation) of $dN/d\log(d_p)$ variables in PC_k . Factor loadings of PC_k represent these coefficients scaled by the λ_k explained by PC_k . Loadings of PC_k thus represent the relative weight of $dN/d\log(d_p)$ variables in PC_k re-scaled by the λ_k explained by PC_k . Factor scores of PC_k are the transformed variables corresponding to a particular data point in the time series of the $dN/d\log(d_p)$ variables. Factor scores thus represent the PC_k values corresponding to each particular data point of the $dN/d\log(d_p)$ time series.

Weekly diurnal cycles, and loadings of PC1-4 are illustrated in Supplementary Figure 2. PC1, PC2, and PC4 represent primary aerosol sources. PC1 is a fine-mode BC aerosol: it correlates to BC, inversely to f_{44} (the lower f_{44} , the more the aerosol approaches the hydrocarbon-like OA), the PNSD mode peaking from 100 to 200 nm. PC2, and PC4 are ultrafine primary aerosols (both correlate to BC primary aerosol (all correlated to BC and f_{BC} ; their PNSD modes peaking from 20 to -). PC1 and PC4 are both sourced by traffic emissions, diurnal cycles peaking at rush hours and week-days. PC1 is a fine mode aerosol component (the PNSD mode peaking from 100 nm, and from 10 to 200 nm), PC4 an ultrafine aerosol component (PNSD peaking from 20 to 40 nm, respectively). PC2 is an ultrafine BC aerosol component, as PC4. Unlike PC4, however, PC2 higher scores are at night-time, and there is no weekly cycle and no peak at "rush hours": PC2 is probably sourced by heating emissions.

The remaining PC3 (more than 10% of the variance) relates to a secondary aerosol: it. It is the only PC inversely correlated to f_{BC} , and directly correlated to f_{OA} , f_{44} , OA-to-BC, and $d_{med(S)}$. Figure 1 shows the PNSD "mode" of this PC, with higher scores at daytime and during week days, the PNSD peaking in the accumulation mode (Supplementary Fig.2). To enhance the interpretation of the aerosol type represented by this PC, Fig. 1 shows its factor loadings (brown line). The PNSD mode of PC3 is exactly the same as that identified by Costabile et al. (2009) for the aerosol "in comparison to those of a PC from a previous study (Costabile et al., 2009), which has very similar statistical properties. This PC was found to represent the droplet mode aerosol. The droplet mode "is a submode of the accumulation mode, resulting from the activation of condensation mode particles to form cloud/fog drops, followed by aqueous-phase chemistry, and droplet evaporation (John, 1990; Meng and Seinfeld, 1994; Seinfeld and Pandis, 2006; Ervens et al., 2011). To our knowledge, the work by Costabile et al. (2009) is the only work in literature showing a similar PC to compare with: authors based its interpretation on five PCAs calculated on a two year dataset over eight concurrent measurement sites, correlated to meteorological and air quality data (green, blue, red, and black lines in Fig. 1.1 indicate the droplet mode PC identified by these five PCAs, calculated by varying the dataset time length and number of measurement sites). The broad similarities between this PC and PC3 allow to deduce with a reasonable statistical accuracy that PC3 does represent the droplet mode aerosol"droplet mode-, as well. This comparison ultimately demonstrates that the "is one of the two aerosol accumulation modes (the smaller one is the condensation mode, brown"

aerosol is secondary in origin (the larger one is the droplet mode), shown to form from activation of condensation mode particles, formation of cloud/fog drops, followed by aqueous-phase chemistry, and droplet evaporation (John, 1990; Meng and Seinfeld, 1994; Seinfeld and Pandis, 2006)-is secondary in origin, because formed through secondary processes in the atmosphere (John, 1990; Meng and Seinfeld, 1994)), and gives insights into its likely formation process. This conclusion is reinforced by the correlation with f_{44} (Tab. 1).

In Table 1, it is indicated a robust statistical relation linking AAE, this "droplet" mode component (PC3), and OA-to-BC, together with f_{OA} , $d_{med(S)}$, f_{44} and f_{43} . Figure 2 shows this relation. When the droplet mode PC scores positive (PC scores >0 indicate that this aerosol type forms), the AAE is greater than 2.5. Both AAE and droplet mode increase with increasing OA-to-BC, and f_{44} , both indicators of OA aged in the atmosphere (Ng et al., 2010; Bond et al., 2013). Data, therefore, identify a "brown" aerosol type, i.e. an aerosol showing AAE from 2.5 to 6, having high "droplet" mode PC scores. The dependence of this "brown" aerosol on PM_1 major constituents, and relevant ratios, is illustrated in Fig. 3 and Fig. 4, where the brown aerosol formation is indicated by the combined increase of AAE (y-axis) and droplet mode PC score (marker color). This "brown" aerosol formation depends on the organic mass fraction (f_{OA} , Fig.3a), and is inversely correlated to the mass fractions of BC (f_{BC} , Fig.3b), and sulfate (f_{SO_4} , Fig.3c). The dependence on the nitrate mass fraction (f_{NO_3} , Fig.3d) is not obvious, as high AAE values and droplet mode scores are observed for both $f_{NO_3} < 0.05$ and $f_{NO_3} \simeq 0.25$.

The relation between this "brown" aerosol and the BC-to-OA ratio (or its inverse OA-to-BC ratio $= f_{OA}/f_{BC}$) is shown in Fig. 4. Uncertainties of AAE, and BC-to-OA in Fig.4 were calculated propagating uncertainties of PSAP-derived σ_a (Sect.2.2), BC derived by the AAE_{BC} attribution method (Sect.3.1), and AMS-derived OA (Sect.2.3). The area showing the brown aerosol (AAE from 2.5 to 6.6, positive droplet mode PC scores) has high OA-to-BC ratios (note correlation $r = 0.78$ between AAE and OA-to-BC ratio, Table 1). The inverse dependence between this "brown" aerosol formation and the BC-to-OA ratio confirms results of the statistical analysis (correlations with f_{44} and f_{43}) indicating that the brown aerosol is an aged OA. Indeed, it is typical that BC contribution declines, and OA contribution increases, as the smoke aerosol ages in the atmosphere. Relative proportions of BC and OA in the AAE vs BC-to-OA relation are indicated in Supplementary Figure 3. It is shown that the increase in AAE with decreasing the BC-to-OA ratio is not simply due to the decreased contribution of BC. The AAE of the aerosol is indeed dictated by the relative contribution of the OA and BC components. There is a small trend of the lowest AAE values toward 1.5, rather than 1. We explain this if we first consider that the variability from 1 to 1.5 of AAE is within the uncertainty of the instrumentation. And second, if we consider that these low AAE values are at OA values larger than zero (although they are very low ($< 3 \mu g \cdot m^{-3}$, Supplementary Fig.2), and thus with low PSAP errors (Lack et al., 2008). The AAE larger than 1 can hence be due to any spectrally

370 light absorbing material that the AMS could not detect (refractory material, or material in particles smaller than 100 nm and larger than 1 μm).

Taken together, findings finally suggest that the "brown" aerosol type observed in the Po Valley ~~is mainly composed of~~, is secondary in origin and contains aged OA in "droplet" mode particles.

4.2 A case study ~~for the "brown" aerosol~~

375 We present here a case study to visualize main aerosol features of the "brown" aerosol observed. The values of this case study were indicated in Fig. 4 by "*": they represent the highest values of AAE, and droplet mode PC scores observed, and thus a case of brown aerosol formation. Figure 5 (panels a, b, c) compares mean values of volume and mass size distributions measured over the whole field experiment with relevant values measured during this case study (first of February, 2013 from 380 17:30 to 19:00). Relative humidity (RH) was high ($97.5 \pm 0.4\%$, against a mean value for the winter campaign of $82 \pm 14\%$, and a maximum of 98%), temperature averaged $2.8 \pm 0.0^\circ\text{C}$ (campaign mean value = $3.5 \pm 2.8^\circ\text{C}$). Aerosol vertical profiles from a LD40 ceilometer (Fig. 5d) indicate a foggy day, except for the middle part of the day (from 11:00 to 15:00) when the fog layer is shown to dissipate. The day started with low concentrations of sub-micrometer aerosol particles (Fig. 5e). 385 Coarse mode aerosol particles increased in the early hours of the day, and then decreased, followed by the increase of droplet mode aerosol particles (as indicated by the area in Fig. 5e corresponding to diameters ranging from 500 to 800 nm, and PC3 scores - not shown here). We interpret this as formation of fog drops, followed by droplet evaporation, and aerosol droplet mode formation, a plausible mechanism for formation of this aerosol type (John, 1990; Meng and Seinfeld, 1994; Seinfeld and Pandis, 2006). AAE (Fig. 5f) was significantly higher than its mean value (up to more than 6 - unfortunately no data is available before 15:00). Relevant volume size distribution (Fig. 5a) is centered on the droplet mode (d_m from 450 to 700 nm), the peak being more than four times as high as that of the mean value. Mass size distributions of the main constituents of nr-PM₁ (NO₃, organics, and NH₄) are centered around 700 nm of the vacuum aerodynamic diameter (d_{va}). Note 390 that $d_{va} = 700\text{ nm}$ corresponds to $d_m = 468\text{ nm}$ for spherical particles with $\rho_p = 1.5\text{ g}\cdot\text{cm}^{-3}$ in the continuum regime, as d_m and d_{va} are linked by Eq.4 (Seinfeld and Pandis, 2006) :

$$d_{va} = d_m \frac{\rho_p}{\rho_0}. \quad (4)$$

In addition, the organic aerosol mass below $d_{va} = 300\text{ nm}$ was significantly lower than that of the droplet mode, especially when compared to the average field results (Fig. 5c). Relevant absorption 400 and scattering coefficients (not shown here) ranged from 5 to 10 Mm^{-1} , and from 300 to 400 Mm^{-1} , respectively. As shown by this case study, a general feature of the whole field campaign was that the brown aerosol formed in the early afternoon.

5 Discussion in comparison with previous works

In this section, we discuss findings to explore consistency with literature, and put results in a broader perspective.

5.1 The "Brown" aerosol in the ambient atmosphere

In Figure 6, relations illustrated in Fig.3 and Fig. 4 between AAE, f_{OA} , and f_{OA}/f_{BC} = OA-to-BC, are compared to literature. Our results (obtained in urban ambient air) are compared to previous findings obtained under "diluted" urban conditions (airborne, and AERONET columnar observations) (Shinozuka et al., 2009; Russell et al., 2010; Arola et al., 2011) (Shinozuka et al., 2009; Russell et al., 2010), or in combustion chambers experiments (Saleh et al., 2014; Lu et al., 2015).

Figure 6a shows the relation between AAE (y axis), f_{OA} (x axis), SSA (at 530 nm, marker color), and $d_{med(S)}$ (marker size). The Pearson's correlation coefficient (r) is 0.56. Fig. 6a-6a is intended to compare to Russell et al. (2010)'s results, indicated by the black line. These results showed that increasing f_{OA} values are accompanied by increasing AAE values when dust is absent. The pattern of our data is similar, although most of our data points (that are ground in-situ measurements) lie above Russell et al. (2010)'s line (that were airborne measurements), and Shinozuka et al (2009)'s results, indicated by grey lines. Note that grey lines by Shinozuka et al (2009) refer to the SSA bins of 0.90-0.92, 0.96-0.98 and 0.98-1.00. There are broad similarities between the three results. As in the case of Russell et al. (2010)'s and Shinozuka et al (2009)'s work, our data make evident that increasing f_{OA} values are accompanied by increasing AAE values, when dust is absent. However, there are conditions when AAE increases irrespective of f_{OA} . In contrast, when f_{OA} is normalised to f_{BC} (f_{OA}/f_{BC} = OA-to-BC ratio), there is a strong correlation with AAE ($r = 0.78$, Fig. 6b). The increasing OA-to-BC ratio is accompanied by a uniform increase of AAE. As well, there is a weak increase of SSA ($r = 0.56$), and $d_{med(S)}$ ($r = 0.49$). As in Shinozuka et al (2009)'s results for SSA bins 0.98-1.00, it is shown that values of $AAE > 3.5$ are at $SSA > 0.98$ (Fig. 6a). Note values measured during the case study (Fig. 55) indicated by "*". This comparison suggests that: All of them are at these high AAEs. This comparison ultimately shows (i) the consistency of "brown" aerosol formation might be observed by airborne and AERONET observations, as well as by ground measurements, and properties observed from airborne/AERONET, and measured in situ at the ground; (ii) the OA-to-BC ratio indicates this formation, and related AAE increase, better to be a better indicator than f_{OA} does of "brown" aerosol and its large AAE values.

Saleh et al. (2014) used the inverse of OA-to-BC to parametrize the AAE of biomass burning emissions in a combustion chamber experiment. To compare to Saleh et al. (2014)'s and Lu et al. (2015)'s work, panel c of Fig. 6-6 shows AAE versus BC-to-OA (the inverse in log scale of the x axis in Fig. 6b). The line in Fig. 6c indicates Black and grey lines in Fig. 6c indicate Saleh et al. (2014)'s and Lu et al. (2015)'s least-square-fit. A similar pattern is evident, although the highest AAE values

~~observed in our study (up to 6.6) were not obtained in the chamber experiment (up to 3.5). Similar results were confirmed by Lu et al. (2015), respectively. There are similar patterns.~~ Both Saleh et al.

(2014) and Lu et al. (2015) concluded that this dependence of AAE on the BC-to-OA ratio can be observed solely for biomass burning OA, and not for fossil fuel OA. Note that ~~when $AAE > 3.5$, SSA is higher than 0.98~~ (we compare, in Fig.6c, different AAE values. In our work, AAE values are due to the whole dust-free aerosol, thus depending on both BC and OA ($AAE_{BC,OA}$). AAE values of Saleh et al. (2014) and Lu et al. (2015) (AAE_{OA}) come from the wavelength-dependence of OA alone (w_{OA}), excluding contributions from BC (AAE_{OA} values are calculated from w_{OA} based on the relation $AAE=w+1$, valid for small particles in the visible range). The comparison in Fig.6), ~~all values of the case study being associated with these high AAE.~~ c is thus intended to compare patterns only, not absolute values. In the Supplementary Fig.3, AAE_{BC} is plotted together with $AAE_{BC,OA}$ in the AAE vs BC-to-OA plot. This figure is intended to indicate wavelength dependence of OA absorption, and suggest possible AAE_{OA} patterns, increasing with decreasing BC-to-OA, similarly to what observed by Saleh et al. (2014) and Lu et al. (2015).

This comparison strengthens our findings indicating that the "brown" aerosol (i) represents an aerosol aged in the atmosphere, and (ii) is not a freshly emitted aerosol, as it is not observed in a combustion chamber experiment. If Saleh et al. (2014)'s results are confirmed, this comparison suggests that this brown aerosol derives from the processing of biomass burning OA. It is worth noting that the AAE of this secondary ~~brown aerosol would be two times "brown" aerosol would~~ probably be higher than that of the fresh biomass burning OA it likely derives from. Lu et al. (2015)'s experiments similarly suggested that atmospheric processing should not decrease biomass burning OA absorptive properties.

5.2 Spectral optical properties of the "brown" aerosol

~~In this section, we discuss if the "brown" aerosol can be the unambiguously identified by its Cluster analysis of aerosol spectral optical properties. In a previous work, Costabile et al. (2013) obtained a paradigm to classify urban aerosol types, based on a proper combination of their AAE, SSA, and SAE is becoming more and more used to infer information on aerosol type from optical data (e.g.,~~ Bergstrom et al., 2007; Clarke et al., 2007; Yang et al., 2009; Russell et al., 2010; Gyawali et al., 2012; Lee et al., 2012; costabile2013). This analysis holds promise for future aerosol classification from remote optical measurements (e.g., AERONET, satellite). Costabile et al. (2013) assessed spectral optical properties of key aerosol populations through Mie theory: soot, biomass burning, two types of organics, dust and marine particles were simulated through a sectional approach where each of these aerosol types was given a monomodal PNSD and a set of three refractive indices (RIs) in the visible ~~region: SAE was plotted against AAE times dSSA (= SSA spectral variation). In panel (a) of range.~~ Relevant Angstrom Exponents of extinction, scattering, and absorption (EAE, SAE, AAE), SSA and its spectral variation (dSSA) were calculated. It was proved that these aerosol types

separately cluster within a "paradigm" where SAE is on the y-axis, dSSA times AAE is on the x-axis, and SSA is on the z-axis (Fig. 7).

In this section, we show this paradigm for that experimental data of the "brown" aerosol (represented by the experimental data of the droplet mode) in comparison to key urban aerosol types (represented by Mie simulated data). Panel (b) is intended to show the variability of relevant spectral optical properties with varying mass fractions of PM₁ major components.

Figure 7a shows that there is an unequivocal spectral signature in the visible region for the do cluster in this paradigm, as well (Fig. 7), and that the cluster of "brown" aerosol :- (i) AAE from 2.5 to 6, (ii) SSA from 0.9 to 1, always increasing with increasing wavelength (λ), (iii) SAE from 0.5 to 2. This signature is in line with that of the data is separated from all other simulated aerosol types, except that named "large organics". Data of "large organics" and "brown" aerosol do overlap, indicating that they may represent the same aerosol type. In fact, microphysical properties of the aerosol type named "large organic mode organics" (LOM). LOM was obtained by simulating: (i) a monomodal PNSD, the mode were simulated to be same as those of the droplet mode aerosol (i.e., PNSD peaking in the "large" accumulation mode, 300-800 nm size range (like the droplet mode PNSD)). Spectral optical properties of this "large organics" aerosol type were simulated by RIs of spectrally absorbing organic material in the visible region: these RIs, given the broad similarities in Fig. 5a); (ii) spectral refractive indices (k_λ) of $k_{467} = 1.460 - 0.012i$, $k_{530} = 1.454 - 0.008i$, and $k_{660} = 1.512 - 0.0075i$. This comparison suggests to extrapolate k_λ values of LOM for the 7, can be assumed to be those of the "brown" aerosol.

This comparison ultimately allows to infer spectral optical properties of "brown" aerosol. It is reasonable that real k_λ values vary much more than simulated ones: numerical simulations represent pure aerosols (pure aerosols have constant k_λ), while experimental data represent mixed aerosols (mixed aerosols have variable k_λ). However, the resulting average (Table 2), definitely not a purely scattering component. It is worth noting that the value of $k_{530} = 8 \cdot 10^{-3}$ assumed for the "brown aerosol", associated to AAE values from 3 to 6, is fully aerosol is consistent with literature k_{530} values recently reviewed by Lu et al. (2015). This result means that visible light absorption properties by the "brown aerosol" have to be carefully considered, and should not be ignored. for the bulk OA obtained from chemically aged primary aerosol. Supplementary Figure 4 shows the variability of relevant spectral optical properties with varying mass fractions of PM₁ major components.

5.3 A SOA type "brown" aerosol

Findings indicate a relation linking the "brown" aerosol to the aged OA. AMS measurements enable to map OA ageing level by combining f_{43} and f_{44} (Sect. 4.1, and Table 1), representing intensities of the two oxygen-containing ions dominating the OA spectra (see review by Moise et al., 2015). f_{44} has been found to originate from the dissociation in the AMS of oxidised organic molecules (the CO₂⁺ fragment from carboxylic acid groups). f_{43} has been related to non-acid oxidised species (the

510 $C_2H_3O^+$ fragment from aldehydes and ketones), in addition to saturated hydrocarbons (the $C_3H_7^+$ fragment). Figure 8 shows f_{44} plotted against f_{43} , and their relation with the brown aerosol (AAE is data color, the droplet mode PC score is data size). This figure is intended to reproduce the "triangle plot" proposed by Ng et al. (2011, 2010), which encompasses the majority of OA values measured in ambient samples. It is showed that the "brown" aerosol (the largest yellow-to-red markers) lies
 515 in the oxidised OA region, where most of the semi volatile oxidised OA measurements taken at the ground lie (Ng et al., 2010; Crippa et al., 2014). The composition found for this "brown" aerosol (high organics, nitrates and ammonium, Fig.5) is coherent with numerous previous studies showing an OA, nitrates being a likely component), its formation process (involving aqueous phase reactions), and AAEs values, are all coherent with previous studies, which showed increased light absorption
 520 towards UV for SOA particles (Jacobson, 1999; Lee et al., 2013; Song et al., 2013; Zhang et al., 2013; Powelson et al., 2014; Lin et al., 2014; Laskin et al., 2015), and sources, composition, and AAE of light-absorbing soluble organic aerosol in urban areas (Zhang et al., 2013, 2011).

This comparison reinforces our hypothesis that the "brown" aerosol is an aged OA.

6 Summary and conclusions

525 We characterized the nondust aerosol having the strongest spectral dependence of light absorption (as indicated by the Absorption ~~Angstrom~~ Ångström Exponent, AAE) at visible wavelengths in ~~an~~ the urban ambient atmosphere of the Po Valley (Bologna). We defined "brown" this bulk aerosol with brown color (it does not necessarily equate to brown carbon). In situ ground ambient measurements of chemical (HR-ToF-AMS), optical (3- λ nephelometer and PSAP), and micro-physical (SMPS
 530 and APS) aerosol properties were taken, together with ancillary observations (~~including ceilometer retrievals~~).

Findings prove that ~~a the observed "brown" aerosol (AAE from 2.5 to 6) forms in the ambient atmosphere, and that this "brown" aerosol is composed by "droplet" mode particles enriched in aged a secondary aerosol dominated by accumulation mode particles containing organic aerosol (OA) and~~
 535 ~~nitrate. We provide a comprehensive physico-chemical characterisation of this brown aerosol, including its spectral optical properties.~~

~~We first identified a specific aerosol type having high AAE values (2.5-6.6), and called it~~ Conditions ~~when "brown" aerosol dominates the bulk dust-free aerosol were first identified based on AAE values. "brownBrown" aerosol . We investigated its major sources in the urban atmosphere by~~
 540 ~~relating were then investigated by relating these~~ relating ~~AAE to key aerosol populations extracted through a statistical analysis of aerosol size distribution. We then characterised physico-chemical statistically identified. Physico-chemical properties of this "brown" aerosol as regards aerosol were characterised:~~
 number and mass size distribution (~~and relevant modes~~), major PM₁ chemical components (BC, organics, nitrate, ammonium, and sulfate), their mass fractions, and relevant ratios (including the BC-

545 to-OA ratio). A case-study was illustrated. ~~It turned out that~~ Overall, the "brown" aerosol ~~÷ (i) is a "droplet" mode aerosol (its monomodal number size distribution peaking at 450-700 nm), (ii) is aged OA, and (iii) can be identified by higher values of the~~ has AAE values from 2.5 to 6, is secondary in origin, formed by the larger accumulation mode particles referred to in literature as droplet mode particles, and contains large concentrations of organic aerosol (OA), its OA-to-BC
550 ratio ~~÷ being higher. Nitrate is an additional likely component.~~

To our knowledge, no previous work has considered these issues in the ambient atmosphere. This is the first experimental evidence that extends observations by Saleh et al. (2014) to ambient conditions, and provides a micro-physical characterization of this "brown" aerosol.

Consistency of findings with literature was then explored. We compared our results with previous
555 findings obtained for "diluted" urban aerosols (airborne and AERONET observations), and freshly emitted aerosols (combustion chamber experiments). We found a dependence of AAE on OA similar to what found for airborne and AERONET data, and a dependence of AAE on the BC-to-OA ratio similar to what found for freshly emitted aerosols. Our study adds to these previous studies that: (i) AAE depends on the OA-to-BC ratio more than on OA, and (ii) the link between AAE and the OA-
560 to-BC (already observed for the freshly emitted primary aerosol from biomass burning) is observed in the ambient atmosphere, as well, where it can be used to identify the "brown" aerosol. Finally, the comparison with a simulation work allowed to obtain the following optical signature in the visible region for the "brown" aerosol: AAE of 2.5-6.6, SAE of 0.5-2, SSA of 0.9-1, and average refractive index at 467 nm of 1.460-0.012i.

565 Findings will have important atmospheric implications for modeling studies, and remote sensing observations. The link between AAE and the OA-to-BC ratio can be a strong tool to parametrize the "brown" aerosol in the atmosphere, as well as to investigate brown OA and Brown Carbon. It is worth noting that this link can be used to extrapolate preliminary chemical information from optical ones, as optical techniques are increasingly used to characterise aerosol properties.

570 *Acknowledgements.* This work was realized in the framework of the Supersito Project. The work was partly accomplished in the framework of the DIAPASON ("Desert-dust Impact on Air quality through model-Predictions and Advanced Sensors ObservatioNs") project, funded by the European Commission (LIFE+ 2010 ENV/IT/391).

References

- Andreae, M. O. and Gelencsér, A.: Black carbon or brown carbon? The nature of light-absorbing carbonaceous aerosols, *Atmos. Chem. Phys.*, 6, 3131-3148, doi:10.5194/acp-6-3131-2006, 2006.
- Arola, A., Schuster, G., Myhre, G., Kazadzis, S., Dey, S., and Tripathi, S. N.: Inferring absorbing organic carbon content from AERONET data, *Atmos. Chem. Phys.*, 11(1), 215-225, 2011.
- Backman, J., Virkkula, A., Vakkari, V., Beukes, J. P., Van Zyl, P. G., Josipovic, M., Piketh, S., Tiitta, P., Chiloane, K., Petäjä, T., Kulmala, M., and Laakso, L.: Differences in aerosol absorption Ångström exponents between correction algorithms for a particle soot absorption photometer measured on the South African Highveld, *Atmos. Meas. Tech.*, 7, 4285-4298, doi:10.5194/amt-7-4285-2014, 2014.
- Bahadur, E., Praveen, P. S., Xu, Y., and Ramanathan, V.: Solar absorption by elemental and brown carbon determined from spectral observations, *P. Natl. A. Sci.*, 109, 17366-17371, 2012.
- Bellouin, N.: Aerosols: The colour of smoke, *Nat. Geosci.*, 7(9), 619-620, 2014.
- Bergstrom, R. W., Russell, P. B., and Hignett, P.: Wavelength Dependence of the Absorption of Black Carbon Particles: Predictions and Results from the TARFOX Ex *Atmos. Chem. Phys.*, 13, 10535-10543, 2013 www.atmos-chem-phys.net/13/10535/2013/ D. A. Lack and J. M. Langridge: Attribution of black and brown carbon light absorption 10541 periment and Implications for the Aerosol Single Scattering Albedo, *J. Atmos. Sci.*, 59, 567-577, 2002.
- Bond, T. C., Anderson, T. L., and Campbell, D.: Calibration and intercomparison of filter-based measurements of visible light absorption by aerosols, *Aerosol Sci. Tech.*, 30, 582-600, 1999.
- Bond, T.C., Doherty, S.J., Fahey, D.W., Forster, P. M., Berntsen, T., DeAngelo, B.J., Flanner, M.G., Ghan, S., Kärcher, B., Koch, D., Kinne, S., Kondo, Y., Quinn, P.K., Sarofim, M.C., Schultz, M.G., Schulz, M., Venkataraman, C., Zhang, H., Zhang, S., Bellouin, N., Guttikunda, S. K., Hopke, P. K., Jacobson, M. Z., Kaiser, J. W., Klimont, Z., Lohmann, U., Schwarz, J. P., Shindell, D., Storelvmo, T., Warren, S.G., Zender, C.S.: Bounding the role of black carbon in the climate system: A scientific assessment, *J. Geophys. Res. Atmos.*, 118, 5380-5552, doi:10.1002/jgrd.50171, 2013.
- Costabile, F., Birmili, W., Klose, S., Tuch, T., Wehner, B., Wiedensohler, A., Franck, U., König, K., and Sonntag, A.: Spatio-temporal variability and principal components of the particle number size distribution in an urban atmosphere, *Atmos. Chem. Phys.*, 9, 3163-3195, doi:10.5194/acp-9-3163-2009, 2009.
- Costabile, F., Barnaba, F., Angelini, F., and Gobbi, G. P.: Identification of key aerosol populations through their size and composition resolved spectral scattering and absorption, *Atmos. Chem. Phys.*, 13, 2455-2470, doi:10.5194/acp-13-2455-2013, 2013.
- Costabile, F., Angelini, F., Barnaba, F., Gobbi, G. P.: Partitioning of Black Carbon between ultrafine and fine particle modes in an urban airport vs. urban background environment, *Atmos. Environ.*, 102, 136-144, 2015.
- Crippa, M., Canonaco, F., Lanz, V. A., Äijälä, M., Allan, J. D., Carbone, S., Capes, G., Ceburnis, D., Dall'Osto, M., Day, D. A., DeCarlo, P. F., Ehn, M., Eriksson, A., Freney, E., Hildebrandt Ruiz, L., Hillamo, R., Jimenez, J. L., Junninen, H., Kiendler-Scharr, A., Kortelainen, A.-M., Kulmala, M., Laaksonen, A., Mensah, A. A., Mohr, C., Nemitz, E., O'Dowd, C., Ovadnevaite, J., Pandis, S. N., Petäjä, T., Poulain, L., Saarikoski, S., Sellegri, K., Swietlicki, E., Tiitta, P., Worsnop, D. R., Baltensperger, U., and Prévôt, A. S. H.: Organic aerosol components derived from 25 AMS data sets across Europe using a consistent ME-2 based source apportionment approach, *Atmos. Chem. Phys.*, 14, 6159-6176, doi:10.5194/acp-14-6159-2014, 2014.

- DeCarlo, P. F., Kimmel, J. R., Trimborn, A., Northway, M. J., Jayne, J. T., Aiken, A. C., Gonin, M., Fuhrer, K., Horvath, T., Docherty, K. S., Worsnop, D. R., and Jimenez, J. L.: Field-deployable, high-resolution, time-of-flight aerosol mass spectrometer, *Anal. Chem.*, 78, 8281-8289, 2006.
- Ervens, B., Turpin, B. J., and Weber, R. J.: Secondary organic aerosol formation in cloud droplets and aqueous particles (aqSOA): a review of laboratory, field and model studies, *Atmos. Chem. Phys.*, 11, 11069-11102, doi:10.5194/acp-11-11069-2011, 2011.
- Gyawali, M., Arnott, W. P., Lewis, K., and Moosmüller, H.: In situ aerosol optics in Reno, NV, USA during and after the summer 2008 California wildfires and the influence of absorbing and non-absorbing organic coatings on spectral light absorption, *Atmos. Chem. Phys.*, 9, 8007-8015, doi:10.5194/acp-9-8007-2009, 2009.
- Hinds W.C., *Aerosol Technology*, 2nd, Edition., Wiley, New York, 1999.
- Khlystov, A., Stanier, C., Pandis, S. N.: An Algorithm for Combining Electrical Mobility and Aerodynamic Size Distributions Data when Measuring Ambient Aerosol, Special Issue of Aerosol Science and Technology on Findings from the Fine Particulate Matter Supersites Program., *Aerosol Sci. Tech.*, 38, S1, 229-238, 2004.
- Lack, D.A., Cappa, C.D., Covert, D.S., Baynard, T., Massoli, P., Sierau, B., Bates, T.S., Quinn, P.K., Lovejoy, E.R. and Ravishankara, A.R.: Bias in filter-based aerosol light absorption measurements due to organic aerosol loading: Evidence from ambient measurements. *Aerosol Science and Technology*, 42(12), pp.1033-1041, 2008.
- Lack, D. A. and Langridge, J. M.: On the attribution of black and brown carbon light absorption using the Ångström exponent, *Atmos. Chem. Phys.*, 13, 10535-10543, doi:10.5194/acp-13-10535-2013, 2013.
- Laskin, A., Laskin, J., and Nizkorodov, S. A.: Chemistry of Atmospheric Brown Carbon, *Chem. Rev.*, doi: 10.1021/cr5006167, 2015.
- Lee, A.K.Y., Zhao, R., Li, R., Liggio, J., Li, S.-M., Abbatt, J.P.D.: Formation of light absorbing organo-nitrogen species from evaporation of droplets containing glyoxal and ammonium sulfate, *Environ. Sci. Technol.*, 47 (22), 12819-12826, doi:10.1021/es402687w, 2013.
- Lin, Y.-H., Budisulistiorini, S.H., Chu, K., Siejack, R.A., Zhang, H., Riva, M., Zhang, Z., Gold, A., Kautzman, K.E., Surratt, J.D.: Light-absorbing oligomer formation in secondary organic aerosol from reactive uptake of isoprene epoxydiols, *Environ. Sci. Technol.*, 48 (20), 12012-12021, doi: 10.1021/es503142b, 2014.
- Lu, Z., Streets, D.G., Winijkul, E., Yan, F., Chen, Y., Bond, T.C., Feng, Y., Dubey, M.K., Liu, S., Pinto, J.P., Carmichael, G.R.: Light absorption properties and radiative effects of primary organic aerosol emissions, *Environ. Sci. Technol.*, 49 (8), 4868-4877, doi: 10.1021/acs.est.5b00211, 2015.
- Jacobson, M. Z.: Isolating nitrated and aromatic aerosols and nitrated aromatic gases as sources of ultraviolet light absorption, *J. Geophys. Res. - Atmos.*, 104(D3), 3527-3542, 1999.
- Jimenez, J. L., Jayne, J.T., Shi, Q., Kolb, C.E., Worsnop, D.R., Yourshaw, I., Seinfeld, J.H., Flagan, R.C., Zhang, X., Smith, K.A. and Morris, J.W.: Ambient aerosol sampling using the Aerodyne Aerosol Mass Spectrometer, *J. Geophys. Res. - Atmos.*, 108 (D7), 1984-2012, doi:10.1029/2001jd001213, 2003.
- John, W., Wall, S. M., Ondo, J. L., and Winklmayr, W.: Modes in the size distributions of atmospheric inorganic aerosol, *Atmos. Environ.*, 24A, 2349-2359, 1990.
- Meng, Z. and Seinfeld, J. H.: On the source of the submicrometer droplet mode of urban and regional aerosols, *Aerosol Sci. Tech.*, 20, 253-265, 1994.

- Middlebrook, A. M., Bahreini, R., Jimenez, J. L. and Canagaratna, M. R.: Evaluation of Composition-Dependent Collection Efficiencies for the Aerodyne Aerosol Mass Spectrometer using Field Data, *Aerosol Sci. Tech.*, 46, 258-271, doi:10.1080/02786826.2011.620041, 2012.
- 655 Moise, T., Flores, J. M., Rudich, Y.: Optical Properties of Secondary Organic Aerosols and Their Changes by Chemical Processes, *Chem. Rev.*, 115.10, 4400-4439, doi: 10.1021/cr5005259, 2015.
- Moosmüller, H., Chakrabarty, R. K., Ehlers, K. M., and Arnott, W. P.: Absorption Ångström coefficient, brown carbon, and aerosols: basic concepts, bulk matter, and spherical particles, *Atmos. Chem. Phys.*, 11, 1217-1225, doi:10.5194/acp-11-1217-2011, 2011.
- 660 Ng, N. L., Canagaratna, M. R., Zhang, Q., Jimenez, J. L., Tian, J., Ulbrich, I. M., Kroll, J. H., Docherty, K. S., Chhabra, P. S., Bahreini, R., Murphy, S. M., Seinfeld, J. H., Hildebrandt, L., Donahue, N. M., DeCarlo, P. F., Lanz, V. A., Prévôt, A. S. H., Dinar, E., Rudich, Y., and Worsnop, D. R.: Organic aerosol components observed in Northern Hemispheric datasets from Aerosol Mass Spectrometry, *Atmos. Chem. Phys.*, 10, 4625-4641, doi:10.5194/acp-10-4625-2010, 2010.
- 665 Ng, N. L., Canagaratna, M. R., Jimenez, J. L., Chhabra, P. S., Seinfeld, J. H., and Worsnop, D. R.: Changes in organic aerosol composition with aging inferred from aerosol mass spectra, *Atmos. Chem. Phys.*, 11(13), 6465-6474, 2011.
- [Pöschl, U.: Aerosol particle analysis: challenges and progress. *Anal. Bioanal. chem.*, 375.1, 30-32, DOI 10.1007/s00216-002-1611-5, 2003.](https://doi.org/10.1007/s00216-002-1611-5)
- 670 Powelson, M. H., Espelien, B. M., Hawkins, L. N., Galloway, M. M., De Haan, D. O.: Brown carbon formation by aqueous-phase carbonyl compound reactions with amines and ammonium sulfate, *Environ. Sci. Technol.*, 48(2), 985-993, doi: 10.1021/es4038325, 2014.
- [Quinn, P. K., Bates, T. S., Coffman, D. J., and Covert, D. S.: Influence of Particle Size and Chemistry on the Cloud Nucleating Properties of Aerosols, *Atmos. Chem. Phys.* 8:1714, 2008.](https://doi.org/10.1021/es4038325)
- 675 Russell, P. B., Bergstrom, R. W., Shinozuka, Y., Clarke, A. D., DeCarlo, P. F., Jimenez, J. L., Livingston, J. M., Redemann, J., Dubovik, O., and Strawa, A.: Absorption Ångström Exponent in AERONET and related data as an indicator of aerosol composition, *Atmos. Chem. Phys.*, 10, 1155-1169, doi:10.5194/acp-10-1155-2010, 2010.
- Saleh, R., Hennigan, C. J., McMeeking, G. R., Chuang, W. K., Robinson, E. S., Coe, H., Donahue, N. M., and Robinson, A. L.: Absorptivity of brown carbon in fresh and photo-chemically aged biomass-burning emissions, *Atmos. Chem. Phys.*, 13, 7683-7693, doi:10.5194/acp-13-7683-2013, 2013.
- 680 Saleh, R., Robinson, E. S., Tkacik, D. S., Ahern, A. T., Liu, S., Aiken, A. C., Sullivan, R. C., Presto, A. A., Dubey, M. K., Yokelson, R. J., Donahue, N. M., and Robinson, A. L.: Brownness of organics in aerosols from biomass burning linked to their black carbon content, *Nat. Geosci.*, 7, 647-650, 2014.
- 685 Seinfeld, J. H. and Pandis, S. P.: *Atmospheric Chemistry and Physics*, 2nd edn., John Wiley, New York, USA, 1232 pp., 2006.
- Shapiro, E. L., Szprengiel, J., Sareen, N., Jen, C. N., Giordano, M. R., and McNeill, V. F.: Light-absorbing secondary organic material formed by glyoxal in aqueous aerosol mimics, *Atmos. Chem. Phys.*, 9, 2289-2300, doi:10.5194/acp-9-2289-2009, 2009.
- 690 Shinozuka, Y., Clarke, A. D., DeCarlo, P. F., Jimenez, J. L., Dunlea, E. J., Roberts, G. C., Tomlinson, J. M., Collins, D. R., Howell, S. G., Kapustin, V. N., McNaughton, C. S., and Zhou, J.: Aerosol optical properties

relevant to regional remote sensing of CCN activity and links to their organic mass fraction: airborne observations over Central Mexico and the US West Coast during MILAGRO/INTEX-B, *Atmos. Chem. Phys.*, 9, 6727-6742, doi:10.5194/acp-9-6727-2009, 2009.

695 Song, C., Gyawali, M., Zaveri, R.A., Shilling, J.E., Arnott, W.P.: Light absorption by secondary organic aerosol from α -pinene: Effects of oxidants, seed aerosol acidity, and relative humidity, *J. Geophys. Res.*, 118 (20), 11741-11749, doi: 10.1002/jgrd.50767, 2013.

Virkkula, A., Ahlquist, N. C., Covert, D. S., Arnott, W. P., Sheridan, P. J., Quinn, P. K., and Coffman, D. J.: Modification, calibration and a field test of an instrument for measuring light absorption by particles, *Aerosol Sci. Tech.*, 39, 68–83, 2005.

700 Virkkula, A.: Correction of the calibration of the 3-wavelength Particle Soot Absorption Photometer (3 λ PSAP), *Aerosol Sci. Tech.*, 44, 706–712, 2010.

[Zhang, X., Lin, Y. H., Surratt, J. D., Zotter, P., Prévôt, A. S., Weber, R. J.: Light-absorbing soluble organic aerosol in Los Angeles and Atlanta: A contrast in secondary organic aerosol. *Geophys. Res. Lett.*, 38\(21\), 2011.](#)

705 Zhang, X., Y.-H. Lin, J. D. Surratt, and R. J. Weber: Sources, composition and absorption angström exponent of light-absorbing organic components in aerosol extracts from the Los Angeles Basin, *Environ. Sci. Technol.*, 47(8), 3685-3693, 2013.

TABLES

Table 1. Pearson's correlation coefficients (r) between: Absorption ~~Angström~~-Ångström Exponent (AAE); scores of principal components (PC1-PC4) of particle number size distributions obtained by Principal Component Analysis (PCA); mass fractions of Black Carbon (f_{BC}), organics (f_{OA}), nitrate (f_{NO_3}), sulfate (f_{SO_4}), and ammonium (f_{NH_4}); median diameter of the particle surface size distribution ($d_{med(S)}$); BC mass concentration (BC); organic aerosol (OA) to BC ratio (OA-to-BC); ratio of the AMS signal at m/z 44 and m/z 43 to the total organics AMS signal (f_{44} and f_{43}). Note that PC3 is the "droplet" mode PC.

r	AAE	$d_{med(S)}$	BC	f_{BC}	f_{OA}	OAtBC	f_{NO_3}	f_{SO_4}	f_{NH_4}	f_{44}	f_{43}
AAE		0.48	-0.26	-0.37	0.56	0.78	-0.31	-0.44	-0.41	0.45	0.45
PC1	0.14	-0.02	0.60	0.31	0.08	0.00	-0.1	-0.35	-0.22	-0.20	-0.25
PC2	-0.18	-0.18	-0.01	0.20	0.09	-0.08	-0.15	-0.15	-0.18	-0.07	0.15
PC3	0.67	0.60	-0.35	-0.42	0.64	0.60	-0.35	-0.49	-0.47	0.42	0.67
PC4	-0.13	-0.34	-0.04	0.19	-0.20	-0.14	0.15	0.03	0.16	0.03	0.24
$d_{med(S)}$	0.48		0.22	-0.48	0.38	0.48	-0.12	-0.25	-0.18		

Table 2. Spectral optical properties of the "brown" aerosol in the visible range: AAE, SSA, and SAE (expressed as mean \pm standard deviation and variation range [minimum- maximum value]), and real and imaginary part (k_λ) of the complex refractive index (RI [λ]).

<u>AAE₄₆₇₋₆₆₀</u>	<u>SSA₅₃₀</u>	<u>SAE₄₆₇₋₆₆₀</u>	<u>real part</u>	<u>RI_{λ}</u> <u>k_λ</u>	<u>[λ]</u>
			<u>1.460</u>	<u>$1.2 \cdot 10^{-2}$</u>	<u>[467nm]</u>
<u>3.5 ± 0.8 [2.5-6]</u>	<u>0.97 ± 0.01 [0.92-0.99]</u>	<u>0.8 ± 0.3 [0-2]</u>	<u>1.454</u>	<u>$8 \cdot 10^{-3}$</u>	<u>[530nm]</u>
			<u>1.512</u>	<u>$7.5 \cdot 10^{-3}$</u>	<u>[660nm]</u>

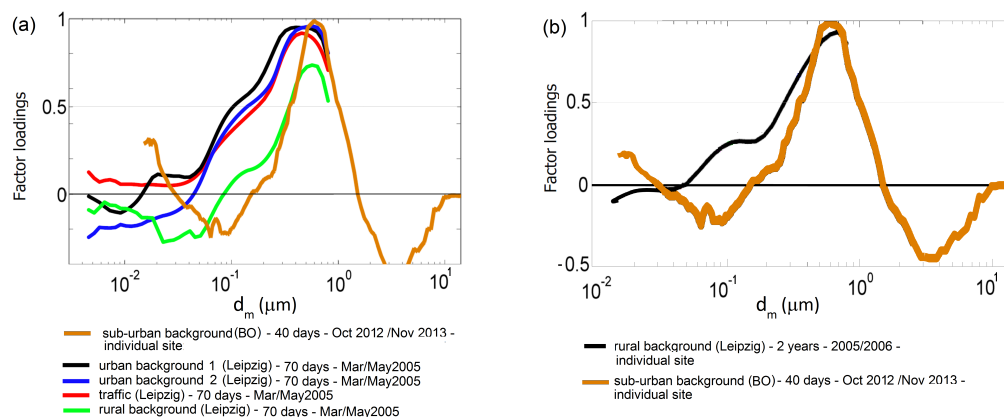


Figure 1. The "droplet" mode of the particle number size distribution (PNSD). Factor loadings calculated by PNSD Principal Component Analysis (PCA) are plotted against electrical mobility particle diameter (d_m). Factor loadings are PCA statistical variables indicating correlations between PNSDs and the droplet mode PCA component. Data from this study (brown line) are compared with data obtained by Costabile et al. (2009) in Leipzig (Germany) at: (a) combined urban sites for 70 days in Spring 2005 (green, blue, red, and black lines, as indicated in the legend), and (b) a single site from long-term (2 years) measurements (black line).

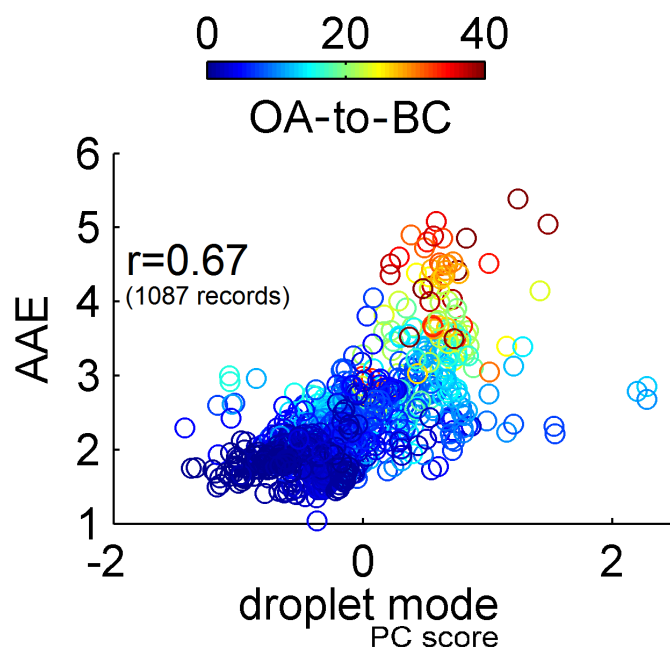


Figure 2. Correlation plot between Absorption ~~Angstrom~~ Ångström Exponent at 467-660 nm (AAE), and the "droplet mode" aerosol (x-axis is the score of the principal component (PC) representing the droplet mode aerosol). Data color is the Organic Aerosol to Black Carbon ratio (OA-to-BC). The Pearson's correlation coefficient (r) is indicated.

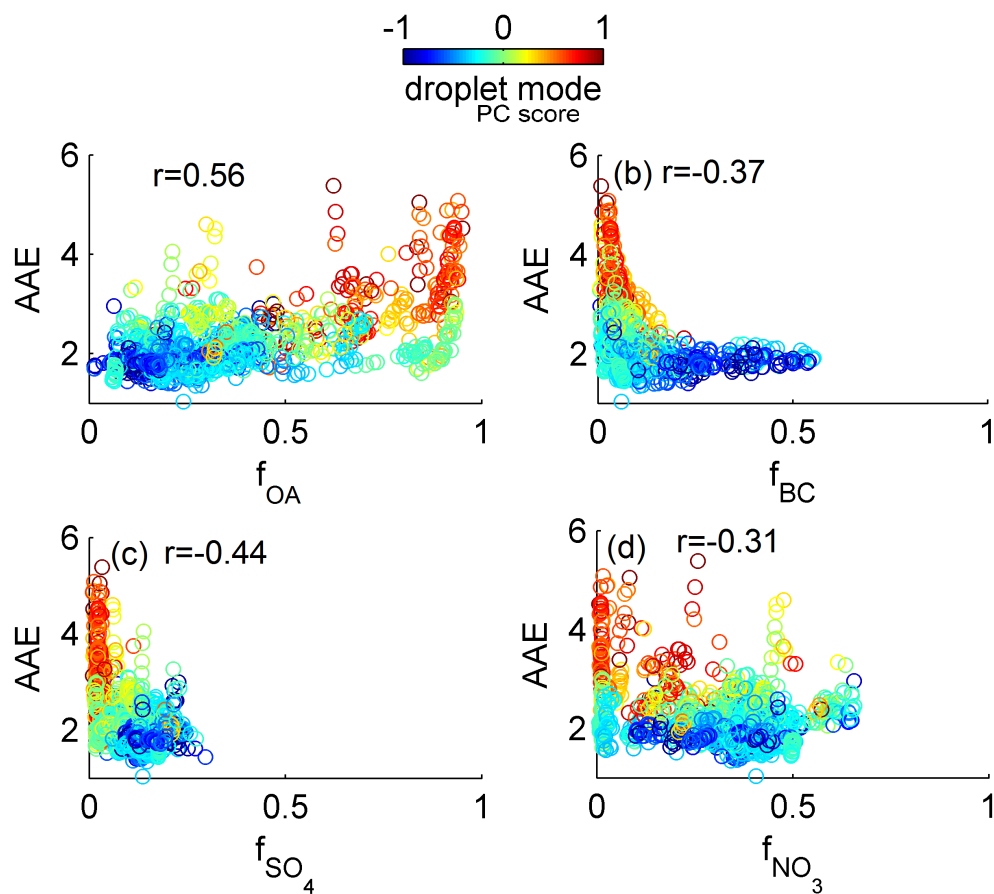


Figure 3. Correlation plots between Absorption ~~Angstrom~~ Ångström Exponent at 467-660 nm (AAE), and mass fractions of (a) organic aerosol (f_{OA}), (b) Black Carbon (f_{BC}), (c) sulfate (f_{SO_4}), and (d) nitrate (f_{NO_3}). Data color is the score of the droplet mode aerosol. Relevant Pearson's correlation coefficients (r) are indicated.

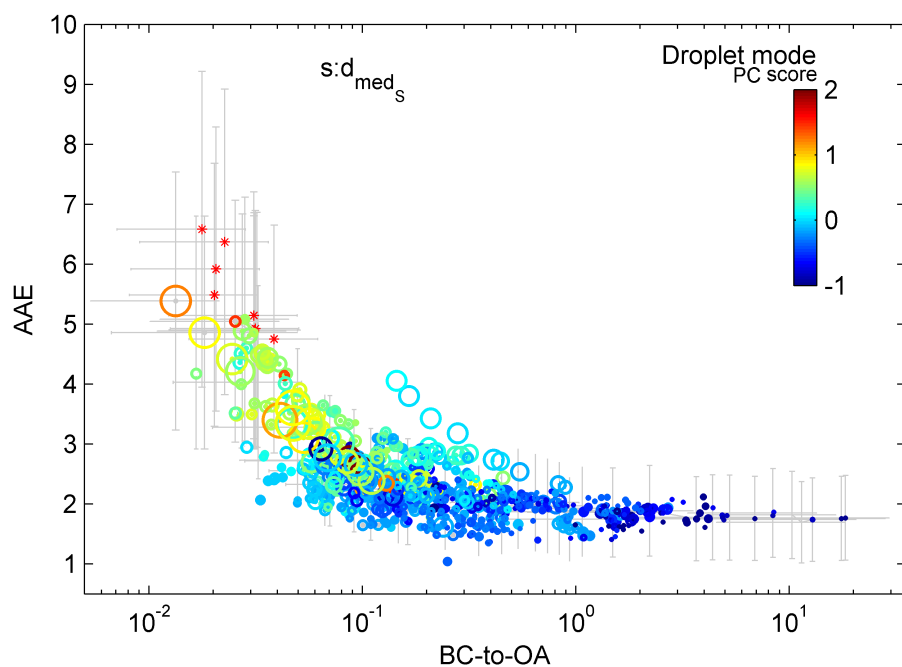


Figure 4. Relation between "brown aerosol" and Black Carbon (BC) to Organic Aerosol (OA) ratio (BC-to-OA). Absorption ~~Angstrom~~ Ångström Exponent at 467-660 nm (AAE) is plotted against BC-to-OA. Data color is the score of the droplet mode PC extracted by the statistical analysis. Data size is the median diameter of the particle surface size distribution ($d_{med(S)}$). Data indicated by "*" show case-study values illustrated in Fig. 5. ~~Grey dots represent all data measured, while colored dots are the subset of these data including statistically significant values of droplet mode PC scores~~ Grey bars indicate measurement uncertainty.

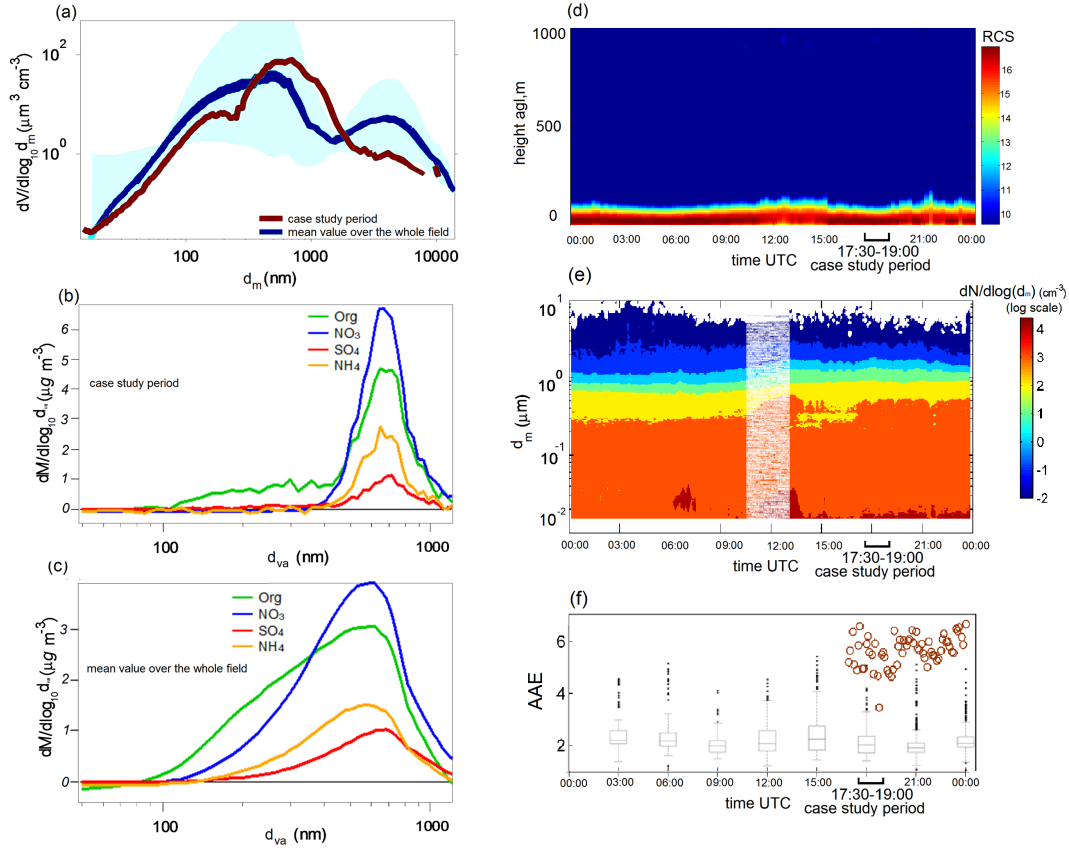


Figure 5. A case-study illustrating major features of the "brown aerosol". Case-study period is the first of February, 2013, from 17:30 to 19:00 UTC. Case-study values are compared with mean values over the whole field experiment. Panels illustrate: (a) particle volume size distribution ($dV/d\log_{10}d_m$, based on electrical mobility particle diameter d_m) during the case-study and relevant mean values; (b) particle mass size distribution ($dM/d\log_{10}d_{va}$, based on vacuum aerodynamic diameter, d_{va}) during the case-study, and (c) relevant mean values; (d) aerosol vertical profiles in the atmosphere during the case-study day (time-height cross section of the range corrected signal, $RCS=\ln(S \times R^2)$, from a LD40 ceilometer); (e) particle number size distributions during the case-study day (whiter area includes corrupted data); (f) Absorption ~~Angstrom-Ångström~~ Exponent at 467-660 nm (AAE) during the case study day (brown circles), and relevant statistical values during the whole field (grey box plots, showing median, percentiles, and outliers).

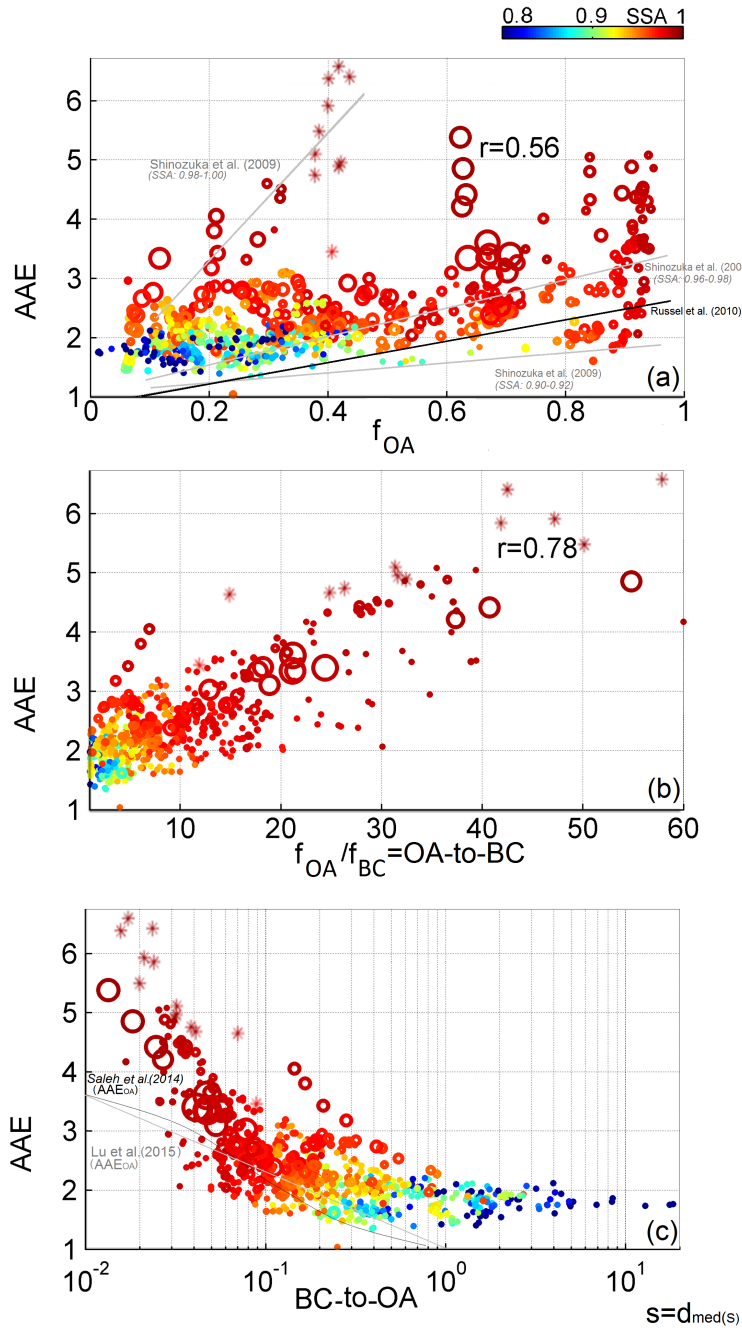


Figure 6. Dependence of Absorption Angstrom-Ångström Exponent at 467-660 nm (AAE) on (a) organic aerosol mass fraction (f_{OA}), (b) Organic Aerosol (OA) to Black Carbon (BC) ratio (OA-to-BC), and (c) BC-to-OA ratio. Data color is Single Scattering Albedo at 530 nm. Data size is median diameter of particle surface size distributions (d_{med} , ranging from 50 to 300 nm). Data indicated by "*" show case study values illustrated in Fig. 5. Relevant Pearson's correlation coefficients (r) are indicated. For comparison, we show previous results: (a) by Russell et al (2010) (black line) and Shinozuka et al. (2009) (grey lines, for the SSA bins of 0.90-0.92, 0.96-0.98 and 0.98-1.00); (c) by Saleh et al.(2014) (black line), and Lu et al (2015) (grey line). Note that AAE includes contributions from both BC and OA, whereas in panel (c), Lu et al (2015) and Saleh et al.(2014) 's results refer to AAE_{OA} only. Previous results by Russell et al (2010) and Saleh et al (2014) are indicated by light lines in panels a and c, respectively.

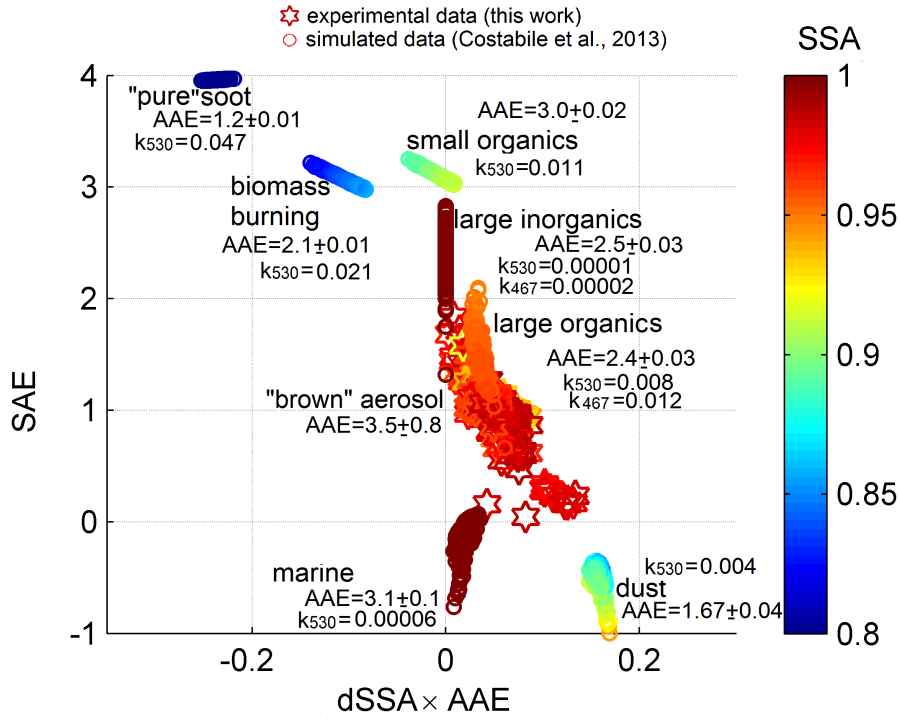


Figure 7. Optical signature of the "brown aerosol" as indicated by the paradigm proposed by Costabile et al. (2013). Absorption ~~Angstrom~~ Ångström Exponent at 467-660 nm (AAE) times spectral variation of Single Scattering Albedo from 660 to 467 nm ($dSSA = SSA_{660} - SSA_{467}$) is plotted against Scattering ~~Angstrom~~ Ångström Exponent at 467-660 nm (SAE). Panel (a) shows experimental data of the droplet mode obtained in this work (representing the brown aerosol) in comparison with key aerosol types obtained through Mie simulations. Data color is SSA at 520 nm. Relevant AAE values for key aerosol types are indicated as mean \pm standard deviation. Panel (b) zooms in panel a to show the "brown" aerosol optical properties variability with varying major PM_{10} mass fractions (f_{OA} , f_{BC} , f_{SO_4} , f_{NO_3}).

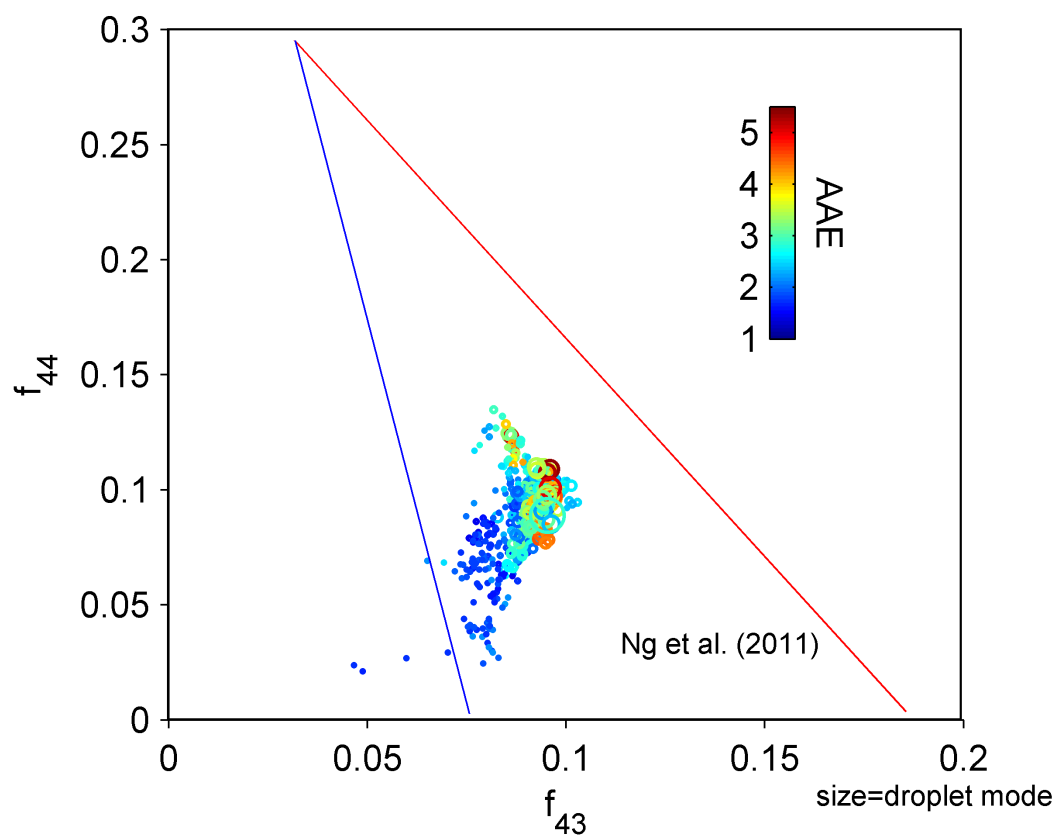


Figure 8. "Triangle plot" reproduced from Ng et al. (2011) for the "brown" aerosol. f_{44} is plotted against f_{43} , data color being the Absorption ~~Angstrom~~ Ångström Exponent at 467-660 nm (AAE), and data size the droplet mode score. The triangular space indicated by red and blue lines shows where the majority of OA values measured in ambient samples fall into.